Broadband Dielectric Spectroscopy on Polymer Blends

12

Huajie Yin and Andreas Schönhals

Contents

Abstract

In this chapter broadband dielectric spectroscopy (BDS) is employed to polymeric blend systems. In its modern form BDS can cover an extraordinary broad frequency range from 10^{-4} to 10^{12} Hz. Therefore, molecular and collective dipolar fluctuations, charge transport, and polarization effects at inner phase boundaries can be investigated in detail including its temperature dependence.

H. Yin • A. Schönhals (✉)
BAM Federal Institute for Materials Research and Testing, Berlin, Germany
e-mail: huajie.yin@bam.de; Andreas.Schoenhals@bam.de

L.A. Utracki, C.A. Wilkie (eds.), *Polymer Blends Handbook*,
DOI 10.1007/978-94-007-6064-6_14,

In the first part of the chapter, the theoretical basics of dielectric spectroscopy are briefly introduced covering both static and dynamic aspects. This section is followed by short description of the various experimental techniques to cover this broad frequency range. To provide the knowledge to understand the dielectric behavior of polymeric blend systems, the dielectric features of amorphous homopolymers are discussed in some detail. This concerns an introduction of the most important relaxation processes observed for these polymers (localized fluctuations, segmental dynamics related to the dynamic glass transition, chain relaxation), a brief introduction to the conductivity of disordered systems as well as polarization effects at phase boundaries. Theoretical models for each process are shortly discussed. In the last paragraph the dielectric behavior of polymer blends is reviewed where special attention is paid to binary systems for the sake of simplicity. In detail the dielectric behavior of binary miscible blends is described. The two most important experimental facts like the broadening of the dielectric relaxation spectra and the dynamic heterogeneity of the segmental dynamics are addressed in depth. Appropriate theoretical approaches like the temperature-driven concentration fluctuation model and the self-concentration idea are introduced.

12.1 Introduction

It was proved by many investigations that broadband dielectric spectroscopy (BDS) is a powerful technique to investigate the properties of polymeric systems (see, for instance, references McCrum et al. 1967; Hedvig 1977; Karasz 1972; Blythe 1979; Williams 1979, 1989, 1993; Runt and Fitzgerald 1997; Adachi and Kotaka 1993; Riande and Diaz-Calleja 2004; Kremer and Schönhals 2003; and references therein). This is mainly due to the fact that an extremely broad dynamical range from the millihertz to the terahertz region can be covered by dielectric spectroscopy in its modern form. A quite recent discussion of the basics and applications of this method can be found in reference Kremer and Schönhals (2003). This broad frequency range of BDS enables one to investigate motional processes which can take place in polymers on quite different length scales (localized fluctuations, segmental dynamics, and motions of the whole chain) by this method in broad range of frequencies and temperatures. This includes furthermore that the molecular motions in the different states of a polymeric material (i.e., the glassy or rubbery state) can be studied in detail from both points of view of basic and applied research. Moreover, the different motional processes as well as charge transport processes depend on the morphology of the system under consideration. Therefore, information on the structural state of the polymeric system under investigation can be indirectly extracted using molecular mobility and/or charge transport as probe for structure.

These considerations are absolutely relevant also for polymeric blends which have received much attention because materials with tailor-made and desired properties can be designed by the combination of polymers with different

properties. Therefore, the purpose of this chapter is to discuss the dielectric properties of polymers with special attention to polymeric blends. The motivation is both scientific and technological.

The literature about dielectric relaxation is rich. For instance, there are several recent reviews available for that field (Simon and Schönhals 2003; Runt 1997; Floudas et al. 2011; Colmenero and Arbe 2007). For instance, by application of dielectric spectroscopy to polymeric blends, the phase behavior of a system can be probed or the degree of miscibility of the blend components in the different phases can be discussed and estimated. This concerns also the question of the dynamic heterogeneity in miscible blend systems or confinement effects in dynamically asymmetric polymer blends (Colmenero and Arbe 2007).

The chapter is organized as follows. In the first part broadband dielectric spectroscopy is introduced. A brief review of the theoretical background of dielectric spectroscopy is provided. This will include the basics of dielectric spectroscopy, dielectric measurement techniques, and also data analysis. This section is followed by a discussion of the dielectric behavior of homopolymers to provide the basics to understand the dielectric properties of blends. In the second part of the chapter, the dielectric behavior of polymeric blends is reviewed where both miscible and immiscible systems are discussed. The chapter is restricted to binary systems.

12.2 Broadband Dielectric Spectroscopy

12.2.1 Fundamentals

Broadband dielectric spectroscopy deals with the interaction of electromagnetic fields with matter. The fundamental relationship between the electric field $\vec{E}$, the magnetic field strength $\vec{H}$, the dielectric displacement $\vec{D}$, the magnetic induction $\vec{B}$, the current density $\vec{j}$, and the density of charges ρ is given by the Maxwell equations (Maxwell 1865, 1868). In the linear case, this means for small electric field strengths, $\vec{D}$ can be expressed by

$$\vec{D} = \varepsilon^* \varepsilon_0 \vec{E}, \tag{12.1}$$

where ε_0 is the dielectric permittivity of vacuum ($\varepsilon_0 = 8.854\ 10^{-12}$ As V^{-1} m^{-1}). The material properties are characterized by the complex dielectric function or dielectric permittivity ε^*. ε^* is time (or frequency) dependent if time-dependent processes take place within the sample. The molecular origin of the time dependence of ε^* will be discussed later during the course of this chapter.

In general, time-dependent processes within a material lead to a difference of the time dependencies of the outer electric field $\vec{E}(t)$ and the resulting dielectric

displacement $\vec{D}(t)$. In the simple case of a periodical field $E(t) = E_0 \exp(-i\,\omega\,t)$ (ω-radial frequency, $\omega = 2\pi f$, f-technical frequency, $i = \sqrt{-1}$ – imaginary unit) in the stationary state, the difference in the time dependence of $\vec{E}(t)$ and $\vec{D}(t)$ is a phase shift which can be described by the complex dielectric function

$$\varepsilon^*(\omega) = \varepsilon'(\omega) - i\varepsilon''(\omega), \tag{12.2}$$

where $\varepsilon'(\omega)$ is the real part and $\varepsilon''(\omega)$ the imaginary part of the complex dielectric function.

Equation 12.1 contains contribution to the dielectric displacement coming from the vacuum. The polarization $\vec{P}$ describes the dielectric displacement which originates from the response only of a material to an external field. It is defined as

$$\vec{P} = \vec{D} - \vec{D}_0 = (\varepsilon^* - 1)\,\varepsilon_0\,\vec{E} = \chi^*\varepsilon_0\,\vec{E} \quad \text{with } \chi^* = (\varepsilon^* - 1), \tag{12.3}$$

where χ^* is the dielectric susceptibility of the material under the influence of an outer electric field. For higher field strengths ($>10^6$ V/m, this order of magnitude will be valid for the most conventional polymeric systems), nonlinear effects may take place which can be described by a Taylor expansion of $\vec{P}$ with regard to $\vec{E}(t)$ where only odd powers will contribute. The corresponding coefficients are called hyperpolarizabilities. For more details, see, for instance, reference Schönhals and Kremer (2003c).

Analogous to Eq. 12.1, Ohm's law

$$\vec{j} = \sigma^*\,\vec{E} \tag{12.4}$$

gives the relationship between the electric field and the current density $\vec{j}$ (Ohm's law) where $\sigma^*(\omega) = \sigma'(\omega) + i\,\sigma''(\omega)$ is the complex conductivity where σ' and σ'' are the corresponding real and imaginary parts, respectively. In the case of absent magnetic fields, the current density and the time derivative of the dielectric displacement are equivalent quantities. It holds

$$\sigma^* = i\,\omega\,\varepsilon_0\,\varepsilon^*. \tag{12.5}$$

The time dependence of the dielectric properties of a material (expressed by ε^* or σ^*) under study can have different molecular origins. Resonance phenomena are due to atomic or molecular vibrations and can be analyzed by optical spectroscopy. The discussion of these processes is out of the scope of this chapter. Relaxation phenomena are related to molecular fluctuations of dipoles due to molecules or parts of them in a potential landscape. Moreover, drift motion of mobile charge carriers (electrons, ions, or charged defects) causes conductive contributions to the dielectric response. Moreover, the blocking of carriers at internal and external interfaces introduces further time-dependent processes which are known as Maxwell/Wagner/Sillars (Wagner 1914; Sillars 1937) or electrode polarization (see, for instance, Serghei et al. 2009).

Because $\vec{D}$ and $\vec{E}$ are vectors, $\varepsilon^*(\omega)$ and σ^* are in general tensors. This becomes important for anisotropic systems like liquid crystalline (Williams 1979) or crystalline materials. For the sake of simplicity, the tensorial character of the dielectric properties is neglected in the further discussion of this chapter.

In the following this chapter is organized as follows. In the first part the essential points of electrostatics are reviewed. That means the dielectric properties are discussed at an infinite time after an application of an outer electric field. In the second part, using the frame of linear response theory, the formalism of time-dependent dielectric processes is developed.

12.2.2 Electrostatics

12.2.2.1 Dipole Moments

The molecular origins of a macroscopic polarization P are dipole moments p_i. Hence, for molecules and/or particles in a volume V, the polarization can be calculated to

$$\vec{P} = \frac{1}{V}\sum \vec{p}_i, \tag{12.6}$$

where i counts all dipole moments in the system. Generally, a dipole moment is created if the electric centers of gravity of positive and negative charges do not collapse. In the simplest case a dipole moment is obtained if a positive and a negative charge q are separated by a distance. Then the dipole moment is $p = q * d$. This picture can be generalized to any distribution of charges (Schönhals and Kremer 2003c).

The microscopic dipole moments can have a permanent or an induced character. In the latter case the dipole moment is induced by the outer electric field itself which distorts a neutral distribution of charges. An example of induced polarization is the electronic polarization where the negative electron cloud of an atom (molecule) is shifted with respect to the positive nucleus. This process takes place at a time constant of 10^{-12} s because of the low mass of the electrons. A further example is atomic polarization which has a comparable time scale. Induced polarization effects can be abstracted in the induced polarization P_∞.

For molecules with a permanent dipole moment μ, charge separation is given by the structure of the chemical compound. Hence, for a system containing only one kind of dipoles, Eq. 12.6 simplifies to

$$\vec{P} = \frac{1}{V}\sum \vec{\mu}_i + \vec{P}_\infty = \frac{N}{V}\left\langle \vec{\mu} \right\rangle + \vec{P}_\infty, \tag{12.7}$$

where N denotes the whole number of dipoles in the system and $<\vec{\mu}>$ the mean dipole moment. If the system contains different kinds of dipoles, one has to sum up over all kinds. This is especially true for polymeric systems where dipole moments

can be related to molecular groups, to segments (repeating unit), or to the chain itself (Schönhals 2003). This will be discussed later during the course of this paragraph.

Permanent dipole moments can be oriented by an electric field. This is called orientation polarization. To calculate the mean dipole moment $<\vec{\mu}>$ under the influence of an electric field, several assumptions must be made. Generally, inertia effects contribute only to P_∞ because of the short time scale involved. Assuming further that the electric field at the locus of the dipole is equal to the outer electric field and that the dipoles do not interact with each other (isolated dipoles), then the mean dipole moment can be calculated in the framework of the Debye approach (Debye 1929). Under these assumptions the mean dipole moment is due to a counterbalance of the thermal energy k_BT (Boltzmann constant) and the interaction energy W of a dipole with the electric field given by $W = -\vec{\mu} \cdot \vec{E}$. Employing Boltzmann statistics and further reconsidering that the electrical interaction energy is small compared to the thermal energy, one obtains (Schönhals and Kremer 2003c)

$$\left\langle \vec{\mu} \right\rangle = \frac{\mu^2}{3\,k_B\,T}\ \vec{E}. \tag{12.8}$$

The polarization can be calculated by inserting Eq. 12.8 into Eq. 12.7:

$$\vec{P} = \frac{\mu^2}{3\,k_B T}\ \frac{N}{V}\ \vec{E}. \tag{14.9}$$

The change in the dielectric permittivity due to orientation polarization can be obtained by combining Eqs. 12.3 and 12.9. It holds

$$\Delta\varepsilon = \varepsilon_S - \varepsilon_\infty = \frac{1}{3\,\varepsilon_0}\ \frac{\mu^2}{k_B\,T}\ \frac{N}{V}, \tag{12.10}$$

where $\varepsilon_S = \lim_{\omega\to 0} \varepsilon'(\omega)$. $\varepsilon_\infty = \lim_{\omega\to\infty} \varepsilon'(\omega)$ covers all contributions to the dielectric function which are due to induced polarization P_∞. In the following $\Delta\varepsilon$ is also called dielectric strength.

The fact that the electric field at the dipole is not exactly the same as the applied one results in shielding effects. These internal field effects were treated historically by Lorentz (1879), Clausius (1879), and Massotti (1847). A more general approach was developed by Onsager (1938) introducing the reaction field. Within this approach Eq. 12.10 is modified to

$$\varepsilon_S - \varepsilon_\infty = \frac{1}{3\varepsilon_0} F \frac{\mu^2}{k_B\,T}\ \frac{N}{V} \text{ with } F = \frac{\varepsilon_S(\varepsilon_\infty + 2)^2}{3\,(2\varepsilon_S + \varepsilon_\infty)}. \tag{12.11}$$

In general the Onsager factor F is an unspecific correction. A more detailed discussion can be found in reference Böttcher (1973).

In difference to the Onsager factor F, the interaction of dipoles plays an important role in condensed systems. This is especially true also for polymeric materials. Specific interactions between molecules and segments in the case of polymers can be caused, for instance, by hydrogen bonding, steric interactions, etc., and can lead to associations of molecules or segments.

The problem of the interaction of dipoles was treated by Kirkwood (1939, 1940, 1946) and Fröhlich (1958). Starting point is the statistical mechanics (Böttcher 1973; Landau and Lifschitz 1979) where the contribution of the orientation polarization to the dielectric permittivity is expressed by

$$\varepsilon_S - \varepsilon_\infty = \frac{1}{3\,k_B\,T\,\varepsilon_0}\,\frac{<\vec{P}(0)\;\vec{P}(0)>}{V} = \frac{1}{3\,k_B\,T\,\varepsilon_0}\,\frac{<\sum_i \vec{\mu}_i(0)\sum_j \vec{\mu}_j(0)>}{V}, \tag{12.12}$$

where $<\vec{P}\,(0)\;\vec{P}\,(0)>$ is the static correlation function of polarization (dipole) fluctuations. The symbol (0) refers to an arbitrary time, for instance, $t = 0$. In the further consideration it is dropped for brevity. The brackets denote averaging which has to be carried out over the whole system considering all interactions. For complex systems including polymers, Eq. 12.12 is extremely difficult to analyze. Therefore, a correlation factor g was introduced by

$$g = \frac{<\sum_i \mu_i \sum_j \mu_j>}{N\,\mu^2} = 1 + \frac{<\sum_i \sum_{i<j} \mu_i \mu_j>}{N\,\mu^2} = \frac{\mu^2_{\text{Interact.}}}{\mu^2}, \tag{12.13}$$

where μ^2 is the mean square dipole moment for noninteracting, isolated dipoles which can be measured, for instance, in diluted solutions. The value of g can be smaller or greater than 1 depending on the case if the segments have the tendency to orient antiparallel or parallel due to specific interaction as discussed above.

The calculation of g by Eq. 12.13 involves the same difficulties as estimations according to Eq. 12.12. Therefore, Kirkwood and Fröhlich (Kirkwood 1939, 1940, 1946; Fröhlich 1958) suggested to treat a given number of dipoles exactly where the remaining molecules/segments were considered like in the Onsager approach as an infinite continuum where the dielectric behavior is characterized by ε_S. Within this approach one obtains

$$\varepsilon_S - \varepsilon_\infty = \frac{1}{3\varepsilon_0} F\,g\,\frac{\mu^2}{k_B T}\,\frac{N}{V}. \tag{12.14}$$

In the simplest case only the nearest neighbors of a selected test dipole are considered. For that case g can be approximated by

$$g = 1 + z < \cos \Psi >, \tag{12.15}$$

where z is the coordination number and ψ is the angle between the test dipole and a neighbor (Böttcher 1973).

12.2.2.2 Dipole Moments of Polymers

For a macromolecule the polarization can be written as

$$\vec{P} = \frac{1}{V} \sum_{\text{chain}} \sum_{\text{repeating unit}} \vec{\mu}_i, \tag{12.16}$$

where $\vec{\mu}_i$ is the dipole moment of the repeating unit i. In difference to low-molecular-weight compounds where the dipole moment can be well represented by a rigid vector for long-chain molecules, there are different possibilities for the orientation of a molecular dipole vector with respect to the polymer backbone. A corresponding nomenclature was developed by Stockmayer (1967) (Stockmayer and Burke 1969). A macromolecule where the dipole moment is oriented parallel to the backbone is called type-A polymer. For these systems the dielectric strength is proportional to the mean square end-to-end vector of the chain (Adachi and Kotaka 1993). For type-B polymers the dipole moment is rigidly attached perpendicular to the chain skeleton. Therefore, for the dipole moment $\vec{P}_B$ of a type-B polymer $< \vec{P}_B \cdot \vec{r} > = 0$ holds, where $\vec{r}$ is the end-to-end vector of the chain, there is no correlation between the dipole moment and the chain contour (no long-range correlations of the dipole moments of different repeating units). Most of the synthetic polymers are of type B. Although there is no polymer which is solely of type-A, there are several examples of macromolecules like *cis*-1,4-polyisoprene (Adachi and Kotaka 1993) having components of the dipole moment parallel and perpendicular to the chain. These polymers are also called type-A or type-AB polymers. A more detailed discussion is given by Adachi (Adachi and Kotaka 1993).

Macromolecules having a flexible side chain carrying a dipole moment are called to be of type C (Block 1979). A typical example are poly(n-alkyl methacrylate)s. This definition is only appropriate under the condition that the side chain can fluctuate on a shorter time scale than the segmental dynamics of the macromolecule. Otherwise the polymer is of type B.

For a type-B polymer, the mean square dipole moment can be expressed by

$$<\mu^2> = \sum_{i=1}^{N} |\vec{\mu}_i|^2 + 2 \sum_{i=1}^{N} \sum_{j<i} |\vec{\mu}_i| \, |\vec{\mu}_j| < \cos \gamma_{ij} >, \tag{12.17}$$

where γ_{ij} is the angle between bonds i and j. $| \vec{\mu} | = m$ denotes the norm of the dipole moment perpendicular to the chain. $<\cos \gamma_{ij}> = 0$ holds for the freely joined

chain model (for definition see Flory (1989)). For real chains also short-range intramolecular correlations ($<\cos\gamma_{ij}> \neq 0$) contribute to the mean square dipole moment which can be described by the intramolecular dipolar correlation coefficient g_{intra} defined as

$$g_{intra} = \frac{<\mu^2>}{\sum_{i=1}^{N} m_i^2} = 1 + 2\sum_{i=1}^{N}\sum_{j<i} <\cos\gamma_{ij}>. \tag{12.18}$$

g_{intra} can be regarded as the Kirkwood/Fröhlich correlation factor for an isolated chain and is a measure for the correlations between dipole moments of neighbored repeating units. Calculations of g_{intra} were started by Debye and Bueche (1951). The rotational isomeric state model (Flory 1989; Volkenstein 1963) can be used to make more detailed estimations. A discussion can be found elsewhere (Riande and Saiz 1992).

12.2.3 Time-Dependent Dielectric Processes

For small electric field strength, the dielectric relaxation can be described in the framework of the linear response theory (Landau and Lifschitz 1979). The relevant materials equation which links the time-dependent polarization P(t) with the time-dependent electric field E(t) is given by (Schönhals and Kremer 2003c)

$$P(t) = P_\infty + \varepsilon_0 \int_{-\infty}^{t} \varepsilon(t-t')\frac{dE(t')}{dt'}dt', \tag{12.19}$$

where P_∞ is the polarization for infinite time covering all contributions from induced polarization and $\varepsilon(t)$ is the time-dependent dielectric function. $\varepsilon(t)$ can be directly measured as response of the system caused by a steplike change of the outer electric field as it is shown in Fig. 12.1.

If the time dependence of the outer electric field is periodically $E^*(\omega) = E_0 \exp(-i\omega t)$, in the stationary case, Eq. 12.19 becomes

$$P^*(\omega) = \varepsilon_0 (\varepsilon^*(\omega) - 1) E^*(\omega), \tag{12.20}$$

where $\varepsilon^*(\omega)$ is the complex dielectric function defined above (see Eq. 12.2). The relationship between $P^*(\omega)$ and $E^*(\omega)$ on the one hand side and $\varepsilon'(\omega)$ and $\varepsilon''(\omega)$ on the other side is sketched in Fig. 12.2. The tangent of the phase angle δ (see Fig. 12.2) is given by

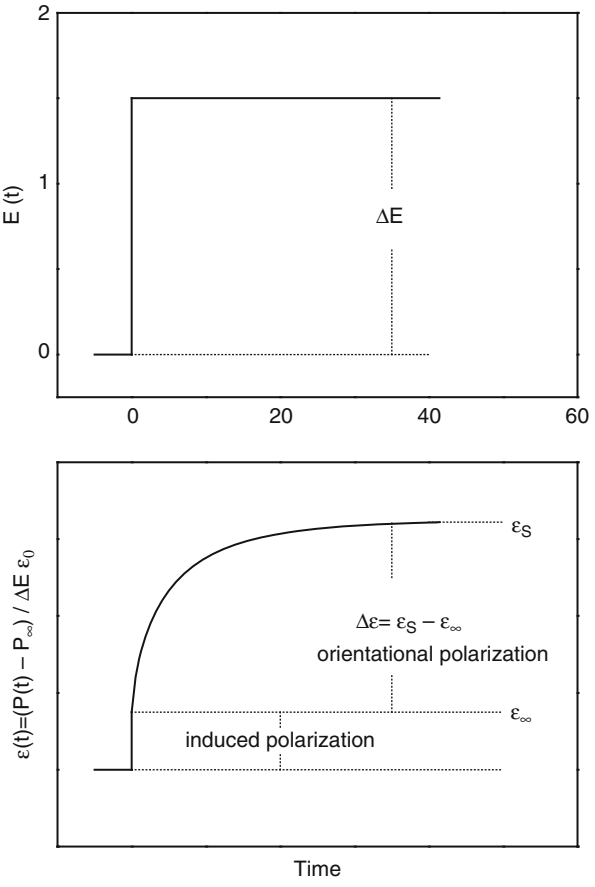

Fig. 12.1 Schematic relationship between the time dependence of the electric field ΔE (*upper panel*), the polarization P(t), and the time-dependent dielectric relaxation function ε(t) (*lower panel*). For the sake of simplicity, the vector sign is omitted in the figure

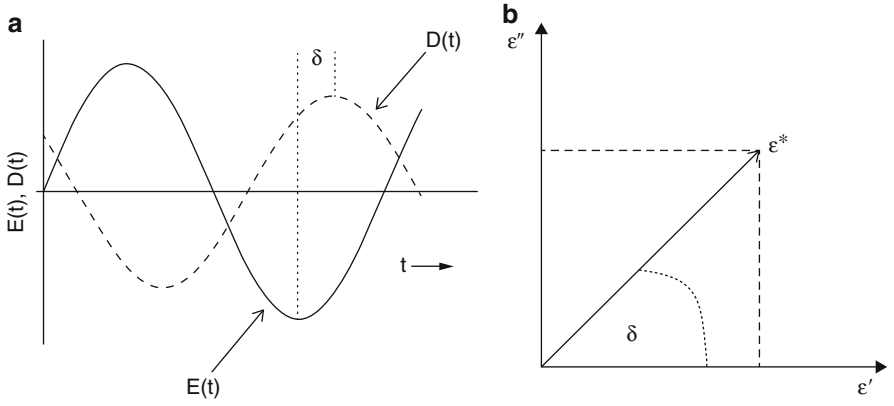

Fig. 12.2 (**a**) Phase shift between the electric field and dielectric displacement. (**b**) Relation between the complex dielectric function, its real part ε′ and imaginary part ε″ as well as the phase angle δ

$$\tan\delta = \frac{\varepsilon''}{\varepsilon'}. \tag{12.21}$$

For scientific studies, however, the dielectric properties should be characterized by $\varepsilon'(\omega)$ and $\varepsilon''(\omega)$ since they have a defined physical significance. In electrical engineering, the reciprocal value of tan δ is termed the merit factor $Q = 1/\tan\delta$.

Equation 12.22 further provides the relationship between the time-dependent dielectric function $\varepsilon(t)$ and the complex dielectric function $\varepsilon^*(\omega)$:

$$\varepsilon^*(\omega) = \varepsilon'(\omega) - i\varepsilon''(\omega) = \varepsilon_\infty - \int_0^\infty \frac{d\varepsilon(t)}{dt}\exp(-i\omega t)\,dt. \tag{12.22}$$

The time dependence of the dielectric response can be due to different processes like the fluctuations of dipoles (relaxation processes), the drift motion of charge carriers (conduction processes), and the blocking of charge carriers at interfaces (Maxwell/Wagner/Sillars polarization). In the following subchapters these effects will be discussed from a theoretical point of view.

12.2.3.1 Dielectric Relaxation

Relaxation processes are due to molecular fluctuations of dipoles. For this case Eq. 12.12 can be generalized to time-dependent processes defining a correlation function $\Phi(\tau)$ by

$$\Phi(\tau) = \frac{<\Delta P(\tau)\,\Delta P(0)>}{<\Delta P^2>} \sim \frac{<\sum_i \vec{\mu}_i(0) \sum_j \vec{\mu}_j(\tau)>}{<\sum_i \mu_i \sum_j \mu_j>}, \tag{12.23}$$

where τ denotes a time variable. It holds $\Phi(0) = 1$ and $\Phi(\tau\to\infty) = 0$. Like Eq. 12.12 $\Phi(\tau)$ can be related to the fluctuations of microscopic dipole moments (right part of Eq. 12.23). For more details see references Williams (1979) and Schönhals and Kremer (2003). Equation 12.23 is difficult to handle from a microscopic point of view.

From a macroscopic point of view, the simplest approach to calculate the time dependence of the dielectric behavior is to assume that the change in polarization is proportional to its actual value (Debye 1929; Fröhlich 1958)

$$\frac{dP(t)}{dt} = -\frac{1}{\tau_D}P(t), \tag{12.24}$$

where τ_D is a characteristic relaxation time. The solution of this first-order differential equation leads to an exponential decay for $\Phi(\tau)$:

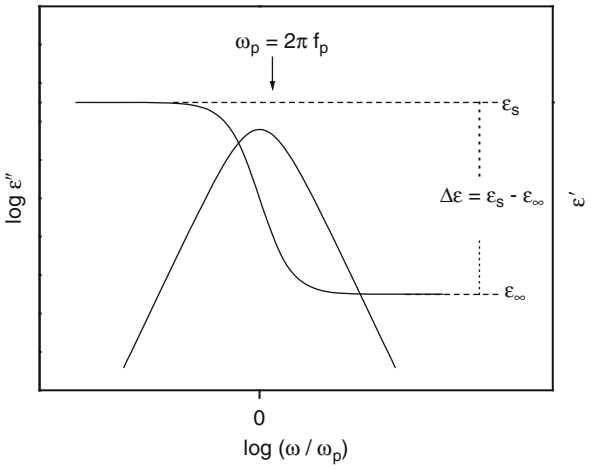

Fig. 12.3 Frequency dependence of the real part ε' and imaginary part ε'' of the complex dielectric function according to the Debye function

$$P(t) \sim \varepsilon(t) \sim \Phi(\tau) = \exp\left[-\frac{t}{\tau_D}\right]. \tag{12.25}$$

According to Eq. 12.22 for the complex dielectric function, one obtains

$$\varepsilon^*(\omega) = \varepsilon_\infty + \frac{\Delta\varepsilon}{1 + i\omega\tau_D};\ \varepsilon' = \varepsilon_\infty + \frac{\Delta\varepsilon}{1 + (\omega\tau_D)^2};\ \varepsilon'' = \frac{\Delta\varepsilon\,\omega\tau_D}{1 + (\omega\tau_D)^2}. \tag{12.26}$$

Equation 12.26 is known as Debye equation. Figure 12.3 gives the frequency dependence of the real and imaginary (loss) part of the Debye function. ε' shows a steplike decay with increasing frequency where ε'' presents a symmetric peak with a maximum $\omega_p = 2\pi f_p = 1/\tau_p$ and a half width of 1.14 decades. The Debye equation can be justified by different molecular models like in the framework of a simple double potential model or the rotational diffusion approach.

For polymeric systems in the most cases, the measured dielectric loss is much broader and in addition the loss peak is asymmetric. This is called non-Debye or nonideal relaxation behavior. Formally such a non-Debye-like behavior can be described by a supposition of Debye functions

$$\varepsilon^*(\omega) - \varepsilon_\infty = \Delta\varepsilon \int_{-\infty}^{\infty} \frac{L(\tau)}{1 + i\omega\tau} d\ln\tau \qquad \int_{-\infty}^{\infty} L(\tau)\, d\ln\tau = 1, \tag{12.27}$$

where $L(\tau)$ is the dielectric relaxation time distribution. A modeling of a dielectric relaxation process by Eq. 12.27 does not mean automatically that the underlying molecular processes can be interpreted in terms of Eq. 12.26.

There were several attempts to generalize the Debye function like the Cole/Cole formula (Cole and Cole 1941) (symmetric broadened relaxation function), the Cole/Davidson equation (Davidson and Cole 1950, 1951), or the Fuoss/Kirkwood model (asymmetric broadened relaxation function) (Fuoss and Kirkwood 1941). The most general formula is the model function of Havriliak and Negami (HN function) (Havriliak and Negami 1966, 1967; Havriliak 1997) which reads

$$\varepsilon^*_{HN}(\omega) = \varepsilon_\infty + \frac{\Delta\varepsilon}{\left(1 + (i\omega\tau_{HN})^\beta\right)^\gamma}. \tag{12.28}$$

In Eq. 12.28 β and γ ($0 < \beta$, $\beta\gamma \leq 1$) are fractional shape parameters which describe the symmetric and asymmetric broadening of the complex dielectric function. τ_{HN} is characteristic relaxation time. The maximum position of the dielectric loss depends on the shape parameters according to (Diaz-Calleja 2000; Boersema et al. 1998; Schröter et al. 1998)

$$\omega_p = \frac{1}{\tau_{HN}} \left[\sin\frac{\beta\pi}{2+2\gamma}\right]^{\frac{1}{\beta}} \left[\sin\frac{\beta\gamma\pi}{2+2\gamma}\right]^{\frac{-1}{\beta}}. \tag{12.29}$$

The separation into real and loss part yield to

$$\varepsilon'(\omega) - \varepsilon_\infty = \Delta\varepsilon\, r(\omega)\cos(\gamma\Psi(\omega)); \quad \varepsilon'' = \Delta\varepsilon\, r(\omega)\sin(\gamma\Psi(\omega)) \tag{12.30}$$

with

$$r(\omega) = \left[1 + 2(\omega\tau_{HN})^\beta \cos\left(\frac{\beta\pi}{2}\right) + (\omega\tau_{HN})^{2\beta}\right]^{\frac{-\gamma}{2}} \tag{12.30a}$$

and

$$\psi(\omega) = \arctan\left[\frac{\sin\left(\frac{\beta\pi}{2}\right)}{(\omega\tau_{HN})^{-\beta} + \cos\left(\frac{\beta\pi}{2}\right)}\right]. \tag{12.30b}$$

Figure 12.4 compares the calculated dielectric loss for the Debye and the HN function for different shape parameters.

From the experimental point of view, all relevant parameters like the relaxation rate (or time), the dielectric strength, and the shape parameters can be estimated by fitting the HN function to the data (for details see references Schlosser and Schönhals 1989; Schönhals and Kremer 2003). As an example Fig. 12.5 gives the dielectric loss for poly(vinyl acetate) at the dynamic glass transition versus frequency at a temperature of $T = 335.6$ K. Only the HN function is able to describe the data correctly.

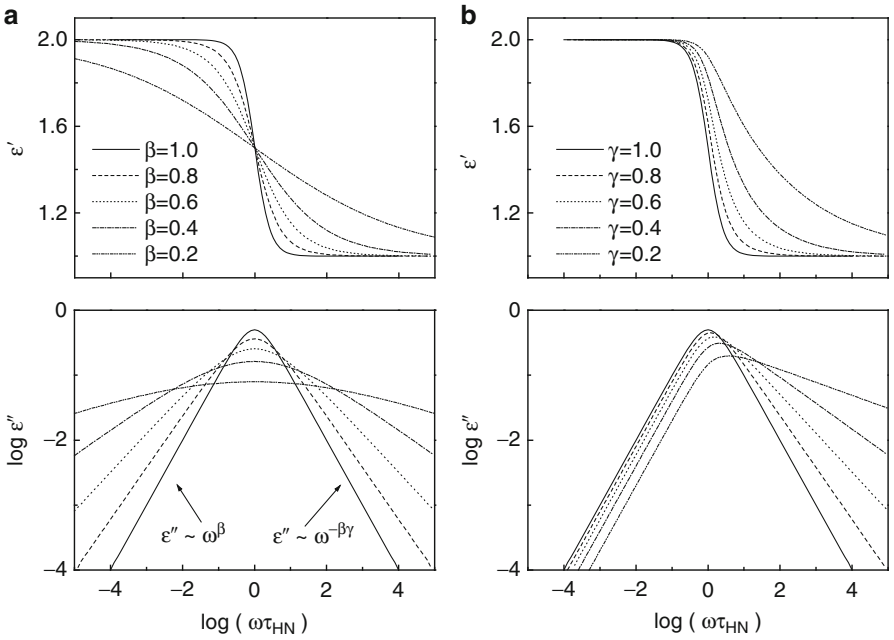

Fig. 12.4 Complex dielectric function according to the Havriliak/Negami function ($\tau_{HN} = 1$ s, $\Delta\varepsilon = 1$, $\varepsilon_\infty = 1$): (**a**) γ fixed to $\gamma = 1$, β varied. (**b**) β fixed to $\beta = 1$, γ varied

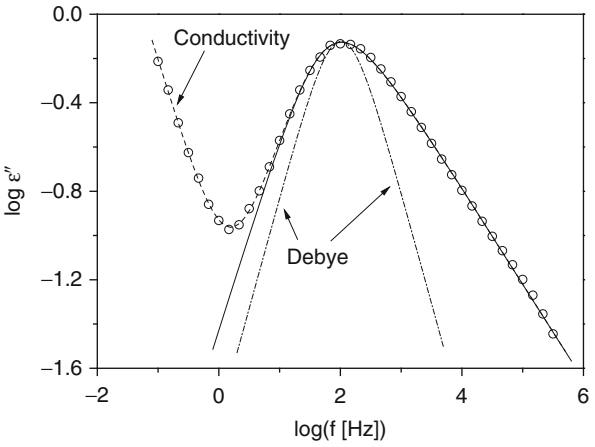

Fig. 12.5 Dielectric loss of poly(vinyl acetate) versus frequency at T = 335.6 K. The *dashed line* is a fit of the HN equation to the data including a conductivity contribution. The *solid line* represents the relaxational contribution according to the HN function. The *dashed-dotted line* represents the Debye function

12.2.3.2 Electrical Conduction

Equation 12.5 gives the relationship between the complex dielectric function and the complex conductivity. For semiconducting disordered materials like conducting polymers, the frequency dependence of the real part of the complex conductivity

$\sigma'(\omega)$ displays a kind of similar behavior (Dyre and Schroder 2000). (1) At temperatures where charge transport is enabled, $\sigma'(\omega)$ has a plateau σ_0 for frequencies ω smaller than a given crossover frequency ω_c. (2) For frequencies $\omega > \omega_c$ a gradual dispersion sets in the form of a power law $\sigma'(\omega) \sim \omega^s$, with $0.5 \leq s \leq 1$. The parameter s increases with decreasing temperature and increasing frequency. (3) In a good approximation a time-temperature superposition can be assumed by scaling the normalized conductivity $\sigma'(\omega)/\sigma'(0)$ with respect to a normalized frequency ω/ω_c. (4) Between $\sigma'(0)$ and ω_c the Barton-Nakajima-Namikawa (BNN) relationship $\sigma'(0) \sim \omega_c$ holds (Barton 1966; Nakajima 1971; Namikawa 1975).

A variety of models exist to explain these similarities on a microscopic level. The simplest of them is the random free energy barrier model developed by Dyre (1988). In this model hopping is assumed to be basic mechanism for conduction where hopping takes place over spatially varying energy barriers. Within the continuous time random walk approximation (Montroll and Weiss 1965), this model results in

$$\sigma^*(\omega) = \sigma(0) \left[\frac{i\omega\tau_e}{\ln(1 + i\omega\tau_e)} \right], \tag{12.31}$$

where $1/\tau_e$ is the attempt frequency to overcome the highest energy barrier determining the DC conductivity $\sigma(0)$. For the real $\sigma'(\omega)$ and imaginary part $\sigma''(\omega)$,

$$\sigma'(\omega) = \frac{\sigma(0)\,\omega\tau_e \arctan(\omega\tau_e)}{0.25\ln^2\left(1 + \omega^2\tau_e^2\right) + \arctan(\omega\tau_e)} \tag{12.32}$$

$$\sigma''(\omega) = \frac{\sigma(0)\,\omega\tau_e \ln(1 + \omega\tau_e)}{0.25\ln^2\left(1 + \omega^2\tau_e^2\right) + \arctan(\omega\tau_e)} \tag{12.33}$$

is delivered. For the exponent s one obtains $s = 1 - 2/\ln(\omega\tau_e)$ (Dyre 1988).

12.2.3.3 Interfacial Polarization

Interfacial polarization or Maxwell/Wagner/Sillars (MWS) polarization (Wagner 1914; Sillars 1937) is a phenomenon that is characteristic for phase-separated or multiphase systems like immiscible polymer blends. Precondition for the observation of a MWS polarization is that the different phases have nonidentical properties. As a result of this, for instance, accumulation of charges takes place at the interfaces of the different phases. Steeman and van Turnhout (2003) published a compilation concerning polymeric materials including polymer blends.

MWS polarization gives rise to a dielectric behavior that can be very difficult to be distinguished from dipole relaxation. All properties of the process related to MWS polarization like its position, its strength, and its shape depend strongly on

the complex permittivity, the geometry and conductivity of the dispersed phase, as well as the dielectric properties of the matrix. As an example, a dispersed phase is considered having the complex dielectric function $\varepsilon_f^*(\omega)$ with the volume fraction ϕ_f where the matrix exhibits a complex dielectric permittivity $\varepsilon_M^*(\omega)$. In a mean field approach, the complex dielectric function $\varepsilon_C^*(\omega)$ of the heterogeneous system can be calculated to (Steeman and van Turnhout 2003)

$$\varepsilon_C^*(\omega) = \varepsilon_M^*(\omega)\frac{\left[n\varepsilon_f^*(\omega) + (1-n)\varepsilon_M^*(\omega)\right] + (1-n)\left[\varepsilon_f^*(\omega) - \varepsilon_M^*(\omega)\phi_f\right]}{\left[n\varepsilon_f^*(\omega) + (1-n)\varepsilon_M^*(\omega)\right] - n\left[\varepsilon_f^*(\omega) - \varepsilon_M^*(\omega)\phi_f\right]}. \quad (12.34)$$

n ($0 \leq n \leq 1$) is the shape factor of the dispersed phase in the direction of the electric field lines. For spheres the values n in three directions (a, b, c) are identical with $n_a = n_b = n_c = 1/3$. For rodlike phase $0 \leq n \leq 1/3$ holds with the limiting case of a needle $n_a = 0$ and $n_b = n_c = 1/2$. For a platelike particle $n_a = 1$ and $n_b = n_c = 0$ holds. For more details see reference van Beek (1967).

Considering these equations one has to keep in mind that the morphology of phase-separated polymer systems is often more complex or even not well defined. This makes a quantitative modeling quite difficult.

12.2.4 Dielectric Instrumentation

The complex dielectric function ε*(f) can be measured in the extremely broad frequency regime from 10^{-3} to 10^{12} Hz. To do so different methods based on different physical principles must be combined. A detailed overview can be found elsewhere (Kremer and Schönhals 2003).

For lower frequencies (10^{-3}–10^{7} Hz), the sample is modeled as a parallel or serial circuit of an ideal capacitor and an ohmic resistor. The spatial extent of the sample on the distribution of the electric field is neglected. This is called lumped circuit approximation. For frequencies higher than 100 kHz, firstly, parasitic impedances caused by cables, connectors, etc., become important. Secondly, the wavelength of the electromagnetic field decreases to the order of magnitude of the sample dimension. This means the geometrical dimensions of the sample capacitor become more and more important limiting the application of the lumped circuit methods to about 10 MHz. For higher frequencies the so-called distributed circuit approach has to be applied. By the application of both waveguide and cavity techniques, complex propagation factor (in reflection or transmission) can be measured from which the complex dielectric function can be deduced in the frequency range from 10^{7} to 10^{11} Hz. For even higher frequencies quasi-optical setups and Fourier transformation techniques can be employed. A detailed discussion of these methods is beyond the scope of this chapter.

The complex dielectric function is related to the complex capacity C* of a capacitor filled with a polymeric material under study by

$$\varepsilon^*(\omega) = \frac{C^*(\omega)}{C_0} = \frac{J^*(\omega)}{i\,\omega\,\varepsilon_0\,E^*(\omega)} = \frac{1}{i\,\omega Z^*(\omega)\,C_0}, \tag{12.35}$$

where C_0 is the (geometrical) capacitance of the unfilled sample capacitor. For a periodical field in the linear range with the angular frequency ω, the complex dielectric function can be expressed by measuring the complex impedance Z*(ω) of the sample where J*(ω) is the complex current density. Different experimental setups (Kremer and Schönhals 2003) like Fourier correlation analysis in combination with dielectric converters (10^{-6}–10^7 Hz) (Pugh and Ryan 1979; Schaumburg 1994, 1999), impedance analysis (10^1–10^7 Hz), RF reflectometry (10^6–10^9 Hz) (Böhmer et al 1989; Jiang et al. 1993), and network analysis (10^7–10^{11} Hz) (Collin 1966; Hewlett Packard 1985; Pelster 1995) are employed. In the following selected methods which have implications on polymeric blend systems are described in more detail.

12.2.4.1 Fourier Correlation Analysis in Combination with Dielectric Converters

The principle of the Fourier correlation analysis is given in Fig. 12.6. A generator provides a sinusoidal voltage $U_1(t)$ with angular frequency ω which causes a current $I_S(t)$ through the sample having an impedance $Z_S^*(\omega)$. The resistor R converts $I_S(t)$ into a voltage $U_2(t)$. Both voltages $U_1(t)$ and $U_2(t)$ are analyzed with respect to their amplitude and phase with regard to the base frequency ω by Fourier analysis. Technically this is carried out by employing two phase sensitive correlators providing the complex voltages $U_1^*(\omega)$ and $U_2^*(\omega)$. Hence, the sample impedance is given according to Ohm's law by

$$Z_S^*(\omega) = \frac{U_S^*(\omega)}{I_S^*(\omega)} = R\left(\frac{U_1^*(\omega)}{U_2^*(\omega)} - 1\right) \tag{12.36a}$$

where for $U_j^*(\omega) = U_j'(\omega) + i\,U_j''(\omega)$ (j = 1,2),

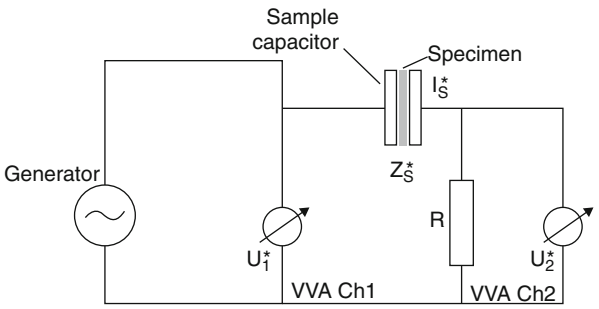

Fig. 12.6 Circuit diagram of Fourier correlation analysis (*VVA* vector voltage analyzer)

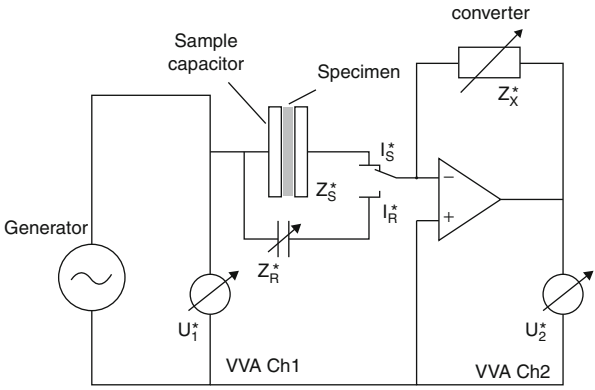

Fig. 12.7 Circuit diagram of Fourier correlation analysis with a dielectric converter for the low-frequency range and a variable reference impedance $Z_R^*(\omega)$ (*VVA* vector voltage analyzer)

$$U_j'(\omega) = \frac{1}{NT}\int_0^{NT} U_j(t)\sin(\omega t)\,dt \quad \text{and} \tag{12.36b}$$

$$U_j''(\omega) = \frac{1}{NT}\int_0^{NT} U_j(t)\cos(\omega t)\,dt \tag{12.36c}$$

holds. N is the number of cycles with duration $T = 2\pi/\omega$, $U_S^*(\omega)$ is the complex voltage at the sample, and $I_S^*(\omega)$ is the complex current through the sample. Technically the Fourier analysis is done by frequency response analyzers or lock-in amplifiers which are state-of-the-art equipments. Digital components like filters are employed.

A fixed resistor R especially for low frequencies f suffers several limitations. Therefore, the resistor R is replaced by an amplifier with a variable gain according to Fig. 12.7. This results in a variable impedance $Z_X^*(\omega)$ which can be adjusted to the impedance of the sample $Z_S^*(\omega)$. For the sample impedance, then

$$Z_S^*(\omega) = \frac{U_{1S}^*(\omega)}{I_S^*(\omega)} = -\frac{U_{1S}^*(\omega)}{U_{2S}^*(\omega)} Z_X^*(\omega) \tag{12.37}$$

holds. The accurateness in the determination of $Z_S^*(\omega)$ is limited by phase and amplitude errors in the amplifier and correlators as well as by the contribution of the cables. These errors can be minimized by measuring a known impedance $Z_R^*(\omega)$ under the same condition as the sample. Analogous to Eq. 12.37

$$Z_R^*(\omega) = \frac{U_{1R}^*(\omega)}{I_R^*(\omega)} = -\frac{U_{1R}^*(\omega)}{U_{2R}^*(\omega)} Z_X^*(\omega) \tag{12.38a}$$

holds. By combining Eqs. 12.37 and 12.38a, one obtains for the impedance of the sample

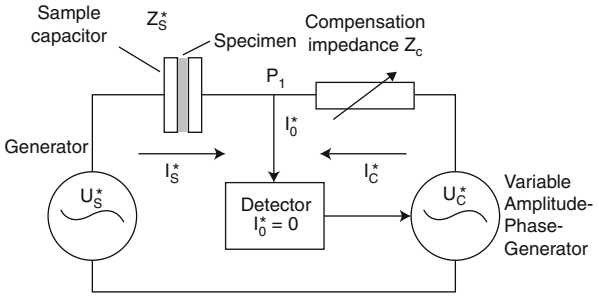

Fig. 12.8 Circuit diagram of an impedance bridge

$$Z_S^*(\omega) = \frac{U_{1S}^*(\omega)}{U_{2S}^*(\omega)} \frac{U_{2R}^*(\omega)}{U_{1R}^*(\omega)} Z_R^*(\omega). \tag{12.38b}$$

12.2.4.2 Impedance Bridges

In principle impedance bridges are the extensions of the Wheatstone resistance bridge to complex resistances (impedances). Historically one has to consider the Schering bridge or the bridge according to Giebe und Zickner (see, for instance, McCrum et al. 1967).

The principle of modern impedance bridges is given in Fig. 12.8. In the sample branch a generator generates the sinusoidal voltage $U_S^*(\omega)$ with an angular frequency ω. This voltage causes a current $I_S^*(\omega)$ through the sample with the impedance $Z_S^*(\omega)$ at point P1. In the comparison branch a second generator generates a voltage which can be varied with regard to both its phase and its amplitude. This voltage is adjusted in that way that it drives a current $I_C^*(\omega)$ through a compensation impedance $Z_C^*(\omega)$ which is equal to $-I_S^*(\omega)$. Hence, in the balanced state at P1 $I_0^* = I_S^* - I_C^* = 0$ is valid and for the sample impedance

$$Z_S^*(\omega) = \frac{U_S^*(\omega)}{I_S^*(\omega)} = -\frac{U_S^*(\omega)}{U_C^*(\omega)} Z_C^*(\omega) \tag{12.39}$$

is obtained.

12.2.4.3 High-Frequency Methods

For frequencies higher than 10^6 Hz, the electromagnetic waves have to be guided in coaxial waveguides because the use of cables will lead to parasitic losses mainly due to inductivities. Moreover, standing waves may arise at frequencies higher than 10^7 Hz. A modern approach to measure the dielectric properties in the frequency range from 10^6 to 10^9 Hz is coaxial reflectometry (Böhmer et al. 1989; Jiang et al. 1993; Agilent Technologies 2000). By this approach the sample is modeled as a part of the inner conductor of a coaxial short. The principle of this technique is illustrated in Fig. 12.9. The impedance of the specimen is estimated from a complex reflection coefficient Γ^* defined by the ratio of the complex voltages of the incident (U_{Inc}^*) and reflected (U_{Ref}^*) waves:

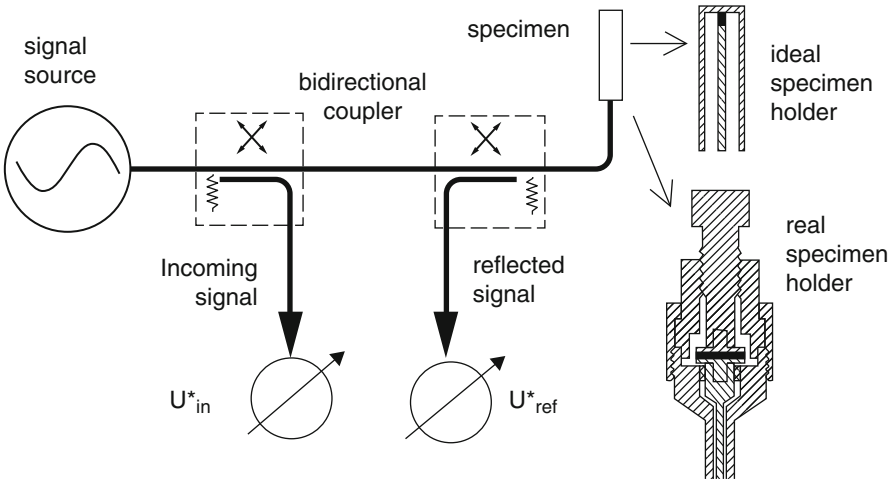

Fig. 12.9 Scheme of a coaxial line reflectometer with sample head

$$\Gamma^* = \Gamma_x - i\,\Gamma_y = \frac{U^*_{Ref}}{U^*_{Inc}} \quad Z^* = Z_0\,\frac{1+\Gamma^*}{1-\Gamma^*}. \tag{12.40}$$

Z_0 is the wave resistance of the coaxial line.

To derive Eq. 12.40 ideal coaxial lines have to be assumed which is not the case in practice. Therefore, calibration procedures have to be applied. First, the influence of the measuring cell has to be obtained and considered during the calculation of the sample impedance. Second, the direction-dependent resistance of the line has to be measured by a second calibration procedure because it cannot be obtained by an equivalent circuit diagram.

At frequencies above 1 GHz, network analysis might be applied where both the reflected and the transmission of the signal through the sample are analyzed with respect to phase and amplitude (Kremer and Schönhals 2003).

An example for a broadband dielectric measurement is given in Fig. 12.10, where the dielectric loss versus frequency is given for poly(propylene glycol) ($M = 200\ g\ mol^{-1}$). The data were obtained by a combination of Fourier correlation analysis and coaxial line reflectometry.

12.2.4.4 Thermostimulated Currents

The dielectric properties of a polymeric system can be also investigated in the temperature domain by the method of thermally stimulated currents (TSC) developed by Bucci et al. (1966). This method was broadly applied to polymers by van Turnhout (1975), Lacabanne (Larvergne and Lacabanne 1993), and Teyssedre (Teyssedre et al. 1997) (see also the references given therein). In principle the method is based on the temperature dependence of the relaxation times and the fact that a given value of the relaxation time corresponds to an experimental time scale

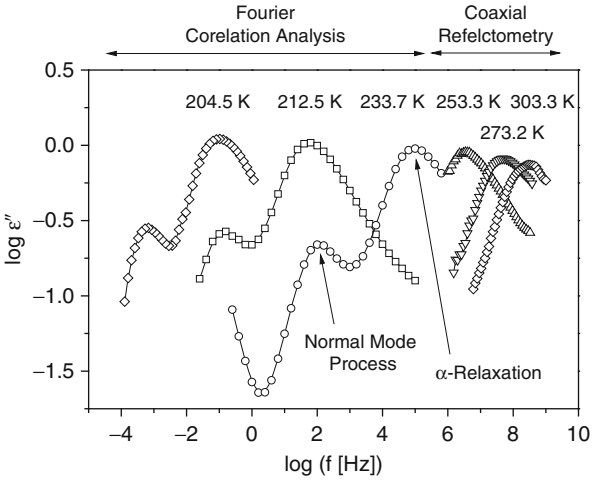

Fig. 12.10 Dielectric loss ε″ versus frequency for poly (propylene glycol) (M = 2,000 g mol^{-1}) at the given temperatures. The peak at lower frequencies corresponds to the normal mode process, whereas the peak at higher frequencies is due to the α-relaxation. The data were obtained by a combination of Fourier correlation analysis and coaxial line reflectometry

(heating rate) at a certain temperature. In the simplest approach assuming a Debye-like response (see Eq. 12.24), the sample is polarized by a field E_P for a given time at a polarization temperature T_P. After that, the sample is cooled down to a temperature T_S with applied electric field. T_S should be low enough that $\tau(T_S)$ is long enough to prevent any depolarization of the sample at the experimental time scale. The frozen-in polarization P_0 is estimated to $P_0 = \frac{N\mu^2}{3k_B T_P V} E_P$. A subsequent heating of the specimen with a heating rate $\kappa = dT/dt$ leads to a depolarization current or depolarization current density J(T). By measuring the current density as function of time, a peak is observed when groups or segments become mobile and frozen-in polarization can be released. According to Eq. 12.24 the temperature dependence of the polarization can be described theoretically by

$$P(T) = P_0 \exp\left(-\int_{T_S}^{T} \frac{dT'}{\kappa\,\tau(T')}\right). \tag{12.41}$$

Experimentally the temperature dependence of the polarization can be obtained by integrating J(T) between T and a temperature T_f at which J(T) becomes zero:

$$P(T) = \frac{1}{\kappa} \int_{T}^{T_f} J(T')\,dT'. \tag{12.42}$$

Depending on the heating rate, a TSD measurement corresponds to a conventional dielectric measurement carried out at a low frequency of 10^{-4}

to 10^{-3} Hz. For this reason a TSC curve can be also directly compared to a corresponding differential scanning calorimetry (DSC) measurement.

A relaxation time can be calculated from the measurements according to (Teyssedre et al. 1997)

$$\tau(T) = -\frac{P(T)}{dP/dT} \tag{12.43}$$

without any further hypothesis.

In addition to these general considerations, methods have been developed considering also a distribution of relaxation times based on partial heating techniques or the fractional depolarization approach (Teyssedre et al. 1997).

Because currents can be measured with a high accuracy, the TCS method is a quick and sensitive method to investigate the dielectric properties of polymers. But it should be noted that, for instance, in the glass transition range, the data depends on the experimental conditions like heating and cooling rates which make the quantitative analysis of these measurements more difficult (Kubon et al. 1988; Schrader and Schönhals 1989).

The application of the TSC method to miscible blends is discussed below (see Sect. 12.4.2). Some further discussion can be found in references Vanderschueren et al. (1980), Topic et al. (1987), Migahed and Fahmy (1994), Topic and Veksli (1993), Sauer et al. (1997), Sauer and Hsiao (1993), and Sauer et al. (1992).

12.3 Dielectric Relaxation of Amorphous Homopolymers

In the following section the essential properties of amorphous polymer systems in the bulk will be discussed briefly. In general, for dense polymers one has to consider that the fluctuations of segments or whole chains are influenced not only by intramolecular but also by intermolecular correlations. In order to calculate the mean square dipole moment (see Eq. 12.16) or the corresponding correlation function, one has to sum up over all chains in the system (Schönhals 2003).

The most amorphous polymers have two relaxation regions. At low temperature (or high frequencies) a so-called β-relaxation is observed as a broad peak in the dielectric loss. At higher temperatures or lower frequencies than the β-process, the α-relaxation is observed which is also called principal relaxation or dynamic glass transition. For type-A polymers (see Sect. 12.2.2.2) having a component of the dipole in the direction of the chain backbone at frequencies lower than that of the α-relaxation, a further dielectric active process is observed which is called α′- or normal mode relaxation related to the overall chain dynamics. As an example for the last two processes, Fig. 12.10 depicts the dielectric loss for poly(propylene glycol) ($M = 2{,}000$ g mol^{-1}) as a type-A polymer in the frequency range from 10^{-4} to 10^{9} Hz. The relaxation processes are indicated as peaks in the dielectric loss. The process at higher frequencies is the α-relaxation which is related to the dynamic

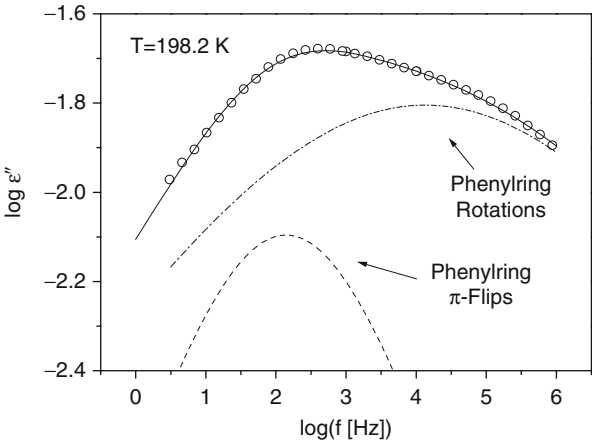

Fig. 12.11 Dielectric loss versus frequency for the β-relaxation of polycarbonate. At a temperature of T = 198.2 K. The *solid line* is a fit of two HN functions to the data where the *dashed* and the *dashed-dotted lines* represent the individual contribution (The figure was adopted from reference Yin et al. (2012))

glass transition, whereas the peak at lower frequencies corresponds to the normal mode process. In the following the characteristic properties of the β-, α-, and the normal mode relaxation of amorphous polymers are briefly discussed. Apart from these processes amorphous polymers can also exhibit further dielectrically active relaxation processes.

12.3.1 β-Relaxation

There is a general agreement that the dielectric β-relaxation of amorphous polymers arises from localized rotational fluctuations of the dipole vector. There are two different approaches to discuss the β-relaxation on a molecular level. At the one hand side, Heijboer (1978) developed a nomenclature for the molecular mechanisms which can be responsible for this process. According to this picture, fluctuations of localized parts of the main chain and the rotational fluctuations of side groups or parts of them can be discussed. There are studies on model systems which seem to support this approach (Buerger and Boyd 1989; Katana et al. 1993; Corezzi et al. 1999; Tetsutani et al. 1982a, b). Moreover, detailed investigations on poly(n-alkyl methacrylate)s in dependence on the length of the alkyl side chain seem to favor this idea also (Tetsutani et al. 1982a, b; Gomes Ribelles and Diaz Calleja 1985; Garwe et al. 1996; Zeeb et al. 1997). Regarding the latter class of materials, one has to keep in mind that the relaxation behavior of the poly(n-alkyl methacrylate)s is quite unusual compared to other polymers. Also a degeneration of the calorimetric glass transition with increasing length of the side chains (Hempel et al. 1996) and indications for a nanophase separation (Beiner and Huth 2003) are detected. Moreover, the β-peak can consist of different relaxation processes. This is demonstrated by Fig. 12.11 where the β-peak of poly(bisphenol A carbonate) is deconvoluted in to two processes (Yin et al. 2012) in agreement also with the literature (Alegría et al. 2006; Arrese-Igor et al. 2008).

The second approach to assign the β-relaxation on a molecular level was outlined by Goldstein and Johari (1970; Johari 1973). In their approach the β-relaxation is a generic feature of the glass transition and the amorphous state. The main argument is that such β-relaxation processes could be observed besides for polymeric systems for a great variety of glass-forming materials like low-molecular-weight glass-forming liquids and rigid molecular glasses (Johari 1973). Also for polymers in which the dipoles are rigidly attached to the main chain, the dielectric β-relaxation was well known. Recently the β-relaxation is intensively discussed because it is supposed that the investigation of this process can help to understand the nature of the dynamic glass transition which is a topical problem of soft matter physics (Anderson 1995; Angell 1995). As a general conclusion one can state that the β-relaxation can be of intra- and/or intermolecular nature.

In the following the properties of the β-relaxation are briefly given in terms of its relaxation rate, its dielectric strength, and the shape of the relaxation function.

12.3.1.1 Relaxation Rate $f_{p,\beta}$

In general the temperature dependence of the relaxation rate of the β-relaxation follows the Arrhenius equation:

$$f_{p,\beta} = f_{\infty\beta} \exp\left[-\frac{E_A}{k_B T}\right]. \tag{12.44}$$

$f_{p\infty}$ is the preexponential factor which should be in the order of 10^{12}–10^{13} Hz. The activation energy E_A depends on both the internal rotational barriers and the environment of a fluctuating unit. Typical values for E_A are 20–50 kJ mol^{-1}.

12.3.1.2 Dielectric Strength $\Delta\varepsilon_\beta$

For most of the polymers for the relaxation strength of the β-relaxation, $\Delta\varepsilon_\beta << \Delta\varepsilon_\alpha$ holds. Here $\Delta\varepsilon_\alpha$ is the dielectric strength of the α-relaxation. This is true for such polymers like polycarbonate (Katana et al. 1993), poly(vinyl chloride) (Matsuo et al. 1965; Colmenero et al. 1993), poly(propylene glycol) (Schönhals and Kremer 1994), or poly(chloroprene) (Matsuo et al. 1965), just to mention a few. This is also the case for semicrystalline polymers poly(ethylene terephthalate) (Coburn and Boyd 1986; Hofmann et al. 1993) or poly(ethylene 2,6 naphthalene dicarboxylate) (Hardy et al. 2001). For some polymers containing flexible side groups like poly(n-alkyl acrylate)s (Kremer et al. 1992; Williams and Watts 1971), $\Delta\varepsilon_\beta \leq \Delta\varepsilon_\alpha$ is valid. The exceptions of these rules are the poly(n-alkyl methacrylate)s for which $\Delta\varepsilon_\beta > \Delta\varepsilon_\alpha$ is measured (McCrum et al. 1967; Garwe et al. 1996; Williams and Edwards 1966; Sasabe and Saito 1968). Untill now the molecular reason for this behavior is not clear. NMR measurements show that the motions of the main and the side chain are coupled (Kulik et al. 1994). This might be a molecular reason for this exception.

12.3.1.3 Shape of the Relaxation Function

The peak related to the β-relaxation is rather broad and symmetric. Using the half-height width of the loss peak, it can be four to six decades wide. With increasing temperature, the width of the β-peak decreases. Quite often the width of the β-relaxation is modeled by both a distribution of the activation energy and the preexponential factor (in the sense of Eq. 12.27) which might be related to a distribution of molecular environments of the relaxing dipole. In most cases it is difficult to extract information on the basic mechanisms of molecular motion. In other cases the broadness of the β-peak can be also due to the overlapping of different relaxation processes as demonstrated for polycarbonate (see Fig. 12.11).

12.3.2 α-Relaxation (Dynamic Glass Transition)

Untill today the dynamic glass transition (α-relaxation) which is related to the thermal glass transition is a topical problem of soft matter research (Anderson 1995; Angell 1995; Schönhals and Kremer 2012). For polymers the dynamic glass transition is related to segmental dynamics which is related to conformational changes. These changes are not independent from each other and many degrees of freedom are involved in such a process. A variety of models have been developed for such a process. Examples for such models are the Shatzki crankshaft (Shatzki 1962) and the so-called three-bond motion (Valeur et al. 1975a, b) which are critically discussed in reference Hall and Helfand (1982). Today, the understanding of the segmental dynamics in an isolated chain is based on ideas of Helfand et al. (Hall and Helfand 1982) and/or Skolnik et al. (Skolnik and Yaris 1982). They describe the segmental motion as a damped diffusion of conformational states along the chain. A conformational transition can occur spontaneously and isolated, but due to the disturbed bond lengths and also the angles, the probability that in a neighbored segment also a conformational transition will take place is enhanced. For this reason a conformational state seems to diffuse along the backbone. At some point this process will stop because of the fact that the probability for a conformation change in a neighbored segment is smaller than one. This means not each conformational change in a segment will lead automatically to a conformational transition in the neighbored unit. So the diffusion of conformational states along the chain is damped.

The model developed for isolated chains in solutions should be also applied in the dense state. But for bulk systems besides the intermolecular interactions, also the intramolecular interactions have to be taken into account. This can be done, for instance, by considering a test segment which fluctuates in the environment of other fluctuating segments (Schönhals and Schlosser 1989).

12.3.2.1 Relaxation Rate $f_{p,\alpha}$

It is well known that the temperature dependence of the relaxation rate of the α-relaxation does not follow the Arrhenius law. Very often close to the thermal

glass transition temperature T_g, it can be described by the Vogel/Fulcher/Tammann/Hesse (VFT) formula (Vogel 1921; Fulcher 1925; Tammann and Hesse 1926):

$$\log f_{p\alpha} = \log f_{\infty\alpha} - \frac{A}{T - T_0}. \tag{12.45}$$

$\log f_{\alpha\infty}$ ($f_{\alpha\infty} \approx 10^{10}$–$10^{12}$ Hz) and A are constants where T_0 is the so-called Vogel temperature which is found to be 30–70 K below T_g. Empirically and also by temperature-modulated DSC (Schick 2012), it was shown that the glass transition temperature corresponds to relaxation rates of 10^{-3}–10^{-2} Hz. Therefore, a dielectric glass transition temperature T_g^{Diel} can be defined by $T_g^{Diel} = T$ ($f_{p\alpha} \approx 10^{-3}...10^{-2}$ Hz).

An analogous representation for the temperature dependence of the relaxation rate of the α-relaxation is the Williams/Landel/Ferry (WLF) relation (Ferry 1980):

$$\log a_T(T) = \log \frac{f_{p\alpha}(T)}{f_{p\alpha}(T_{Ref})} = -\frac{C_1(T - T_{Ref})}{C_2 + T - T_{Ref}}, \tag{12.46}$$

where $a_T(T)$ is the so-called shift factor, T_{Ref} is a reference temperature and $f_{p\alpha}(T_{Ref})$ is the relaxation rate at this temperature. C_1 and $C_2 = T_{Ref} - T_0$ are the WLF parameters. Equations 12.45 and 12.46 are mathematically equivalent. Moreover, it has been discussed that the WLF parameters should have universal material-independent values if $T_{Ref} = T_g$ is chosen (Ferry 1980). However, it was found experimentally that these estimates are only rough approximations.

$a_T(T)$ is often used to construct master curves in the framework of the time-temperature superposition (TTS) principle (Ferry 1980).

The VFT equation can be used to describe the temperature dependence of the relaxation rate close to the glass transition temperature. For higher temperatures ($T = T_g + 80 \ldots 100$ K) deviations are observed. It is discussed in the literature whether the data at higher temperature have to be described by a second VFT law with different parameters or by an Arrhenius equation.

There are several models to understand the strong temperature dependence of the relaxation rate of the dynamic glass transition. Besides mode coupling theory (see, for instance, Götze 2009), one of them is the free volume approach discussed in detail in reference Schönhals and Kremer (2012). The cooperativity approach was pioneered by Adam and Gibbs (1965). They introduced the cooperatively rearranging region (CRR) which is defined as the smallest volume which can change its configuration independently from the neighboring regions. If z(T) is the number of segments per CRR, the relaxation rate can be expressed as

$$\frac{1}{\tau} \sim f_p \sim \exp\left(-\frac{z(T)\,\Delta E}{k_B\,T}\right) \sim \exp\left(-\frac{s^*\Delta E}{k_B T S_C}\right) \sim \exp\left(-\frac{C}{T S_C}\right). \qquad (14.47)$$

ΔE is a free energy barrier for a conformational change of a segment, S_C is the total configurational entropy, and s* is the configurational entropy related to such a rearrangement. The right-hand part of Eq. 12.47 corresponds to the original formulation of Adam and Gibbs theory (Adam and Gibbs 1965). The configurational entropy S_C can be related to the change of the specific heat capacity Δc_p at T_g by

$$S_c(T) = \int_{T_2}^{T} \frac{\Delta c_p}{T}\,dT. \qquad (12.48)$$

With $T_2 = T_0$ and $\Delta c_p \sim 1/T$, the VFT equation is obtained. At the Vogel temperature the configurational entropy vanishes, z(T) diverges like $z(T) \sim (T - T_0)^{-1}$, but no information about the absolute size of a CRR can be obtained. The approach of Adam and Gibbs was extended by Donth (1992, 2001) to obtain the size of a CRR. Within a fluctuation model a formula was developed which allows to calculate a correlation length ξ (or volume V_{CRR}) from the height of the step in c_p and the temperature fluctuation δT of a CRR at T_g as

$$\xi^3 = V_{CRR} = \frac{k_B\,T_g^2 \Delta(1/c_p)}{\rho\,\delta T^2}, \qquad (12.49)$$

where ρ is the density and $\Delta(1/c_p)$ the step of the reciprocal specific heat capacity at the glass transition where $c_V \approx c_p$ was assumed. δT can be extracted experimentally from the width of the glass transition (Donth 1982; Schneider et al. 1981; Donth et al. 2001a, b). Within that approach the size of a CRR was estimated for several polymers to be in the range of 1 to 3 nm in accord with the above estimation. This corresponds to 10–200 segments (Hempel et al. 2000; Beiner et al. 1998b; Kahle et al. 1997).

12.3.2.2 Dielectric strength $\Delta\varepsilon_\alpha$

Generally, for the α-relaxation $\Delta\varepsilon_\alpha$ decreases with increasing temperature. This seems in accord with Eq. 12.11, but the experimental results show that the dependence is much stronger than predicted. Especially close to T_g the increase of $\Delta\varepsilon_\alpha$ with decreasing temperature is quite strong. It is clear that this increase of $\Delta\varepsilon_\alpha$ with decreasing temperature cannot be explained by the increase of the density with decreasing temperature. Also its modeling by a temperature-dependent g-factor remains formal because g was introduced to describe static correlations between dipoles like association. Apart from polymer a similar temperature dependence of $\Delta\varepsilon_\alpha$ was also observed for low-molecular-weight glass-forming materials (Schönhals 2001). It can be argued that this temperature dependence results from

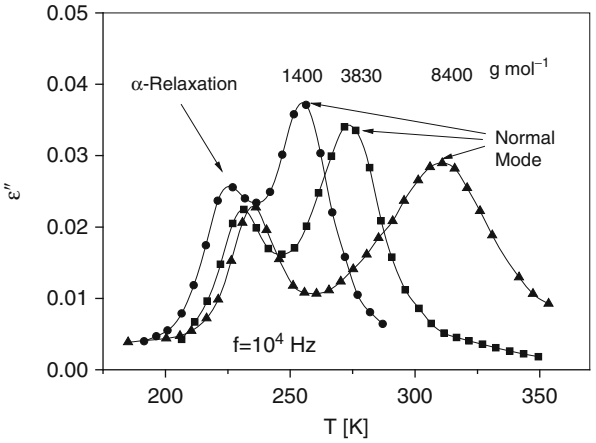

Fig. 12.12 Dielectric loss versus temperature at fixed frequency of 10^4 Hz for *cis*-1,4-polyisoprene. The molecular weights are as follows: *circles*, 1,400 g mol^{-1}; *squares*, 3,830 g mol^{-1}; and *triangles*, 8,400 g mol^{-1}. *Lines* are guides for the eyes (The figure was adapted from Schönhals (1993))

an increasing influence of (intermolecular) cross-correlation terms to μ^2 with decreasing temperature. In other words the reorientation of a test dipole is influenced increasingly by its environment with decreasing temperature. This is in agreement with the cooperativity approach to the glass transition as discussed above.

12.3.2.3 Shape of the Relaxation Function

In general the α-process shows in the frequency domain a broad (the width ranges from two up to six decades depending on structure) and asymmetric peak. Generally, it is assumed that in contradiction to the β-process, the shape of the relaxation function of the dynamic glass transition is not related to a distribution of relaxation times due to local spatial heterogeneities. Rather this broad, asymmetric loss peak is an intrinsic feature of the dynamics of glass-forming systems.

12.3.3 Normal Mode Process

A dielectric normal mode process is observed only for polymers having a dipole moment in parallel to the chain backbone, the so-called type-A polymers like *cis*-1,4-polyisoprene or poly(propylene glycol). The resulting dipole moment is proportional to the end-to-end vector of the chain. Therefore, the normal mode relaxation is directly related to the overall chain dynamics. Figure 12.10 shows that the corresponding relaxation rate $f_{p,n}$ is always located at frequencies lower than that characteristic for the α-relaxation. $f_{p,n}$ depends strongly on the molecular weight of the polymer chain. Figure 12.12 shows the dielectric loss versus temperature at a fixed frequency for *cis*-1,4-polyisoprene for different molecular weights. While the low-temperature (high-frequency) α-relaxation shows only a weak dependence on the molecular weight M, the high-temperature peak caused by the normal mode process depends strongly on M.

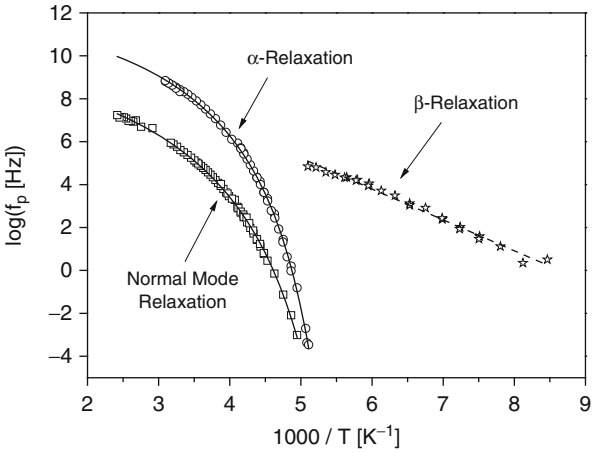

Fig. 12.13 Relaxation rate versus inverse temperature for poly(propylene glycol) (M = 4,000 g/mol): *stars*, β-relaxation; *spheres*, α-relaxation; *squares*, normal mode relaxation. The *dashed line* is a fit of the Arrhenius equation to the data of the β-relaxation. The *solid lines* are fits of the VFT equation to the corresponding data

The temperature dependence of the relaxation rate for the normal mode process follows in a wide temperature range the VFT equation but with different parameters than for the α-relaxation.

For chains with a low molecular weight (unentangled case), the Rouse theory (Adachi and Kotaka 1993; Rouse 1953) can be employed to describe it because excluded volume effects and hydrodynamic interactions are screened out (de Gennes 1979).

For higher molecular weights (entangled case), in principle the reputation theory (de Gennes 1979; Doi and Edwards 1986) and its generalization (contour length fluctuations and/or constrained release) have to be used (Milner and McLeish 1998; Likhtman and McLeish 2002; Liu et al. 2006; Zamponi et al. 2006; Chávez and Saalwächter 2010). A more detailed discussion of the normal mode process is beyond this chapter. The reader is referred to the relevant literature (Adachi and Kotaka 1993; Schönhals 1993; Gainaru and Böhmer 2009; Abou Elfadl et al. 2010).

To conclude this section Fig. 12.13 gives the relaxation map where the relaxation rates for the different processes are plotted versus inverse temperature for poly (propylene glycol) with a molecular weight of 4,000 g mol^{-1}. While the temperature dependence of the β-relaxation follows the Arrhenius equation, the relaxation rates for both the α-process and the normal mode process are curved when plotted 1/T.

12.4 Dielectric Relaxation of Polymer Blends

12.4.1 General Consideration

The blend miscibility is governed by the free energy of mixing:

$$\Delta G_M = \Delta H_M - T\Delta S_M, \tag{12.50}$$

where ΔG_M is the change in the Gibbs free energy of mixing. ΔH_M and ΔS_M denote the excess enthalpy and the mixing entropy. Mixing will take place for $\Delta G_M < 0$.

For polymers the contribution of the entropy of mixing ΔS_M to the free enthalpy of mixing ΔG_M is small. According to the lattice model of Flory/Huggins (Sperling 1986), ΔG_M is assumed to be

$$\Delta G_M = -k_B T \Delta S_M + \kappa \Phi_1 \Phi_2. \tag{12.51}$$

Here Φ_i are the volume fractions, N_i are the degrees of polymerization, and κ denotes the Flory/Huggins interaction parameter. For the entropy of mixing ΔS_M,

$$\Delta S_M = -\left[\frac{\Phi_1}{N_1} \ln \Phi_1 + \frac{\Phi_2}{N_2} \ln \Phi_2\right] \tag{12.52}$$

is assumed. Based on the principle of thermodynamics, the conditions for miscibility, the critical (solution) temperature for phase separation T_C, or the binodals can be calculated from Eqs. 12.51 and 12.52. In general the Flory/Huggins theory can be used to describe systems with an upper critical solution temperature. This means at temperatures above T_C, the two components are miscible on a molecular level, whereas below T_C phase separation occurs. The composition of these phases follows the binodal. That means even in the phase-separated state, a certain degree of mixing (depending on κ and on N_i) is observed which leads to a component 1 and to a component 2 rich phase. Systems with a lower critical solution temperature cannot be described by the Flory/Huggins theory.

Because for most systems the entropy of mixing is small, attractive interactions between both components are needed to obtain a homogeneous mixed state. In the opposite case miscible polymer blends for which $\kappa \approx 0$ (no or weak interactions) are called athermal blends.

In general the β-, the α-, and even the normal mode process will be modified in the case of miscible blends or in systems with partial miscibility. Only for completely phase-separated materials (as the limiting case), the relaxational characteristic of both compounds is fully maintained. The most sensitive process with regard to blending is the α-relaxation. Figure 12.14a shows the expected relaxation map for a miscible system. From the theoretical point of view, a single α-process should be observed which is located – depending on the composition – in between the traces obtained for each component. There are several models like the Flory/Fox or the Gordon/Taylor equation for the dependence of the glass transition temperature on the composition for a homogeneous blend which can be found in standard textbooks of polymer science (Sperling 1986; Strobl 1996). For more theoretical discussion see, for instance, reference Lu and Weiss (1992). A recent comparison is given in reference Brostow et al. (2008). Discussions in the frame of the self-concentration model (for a detailed discussion see below) are given in Lodge and McLeish (2000). This concerns also the Brekner equation (Brekner et al. 1988).

For a phase-separated blend with a partial miscibility, two α-processes will be observed where the location of both processes depends on the composition of both

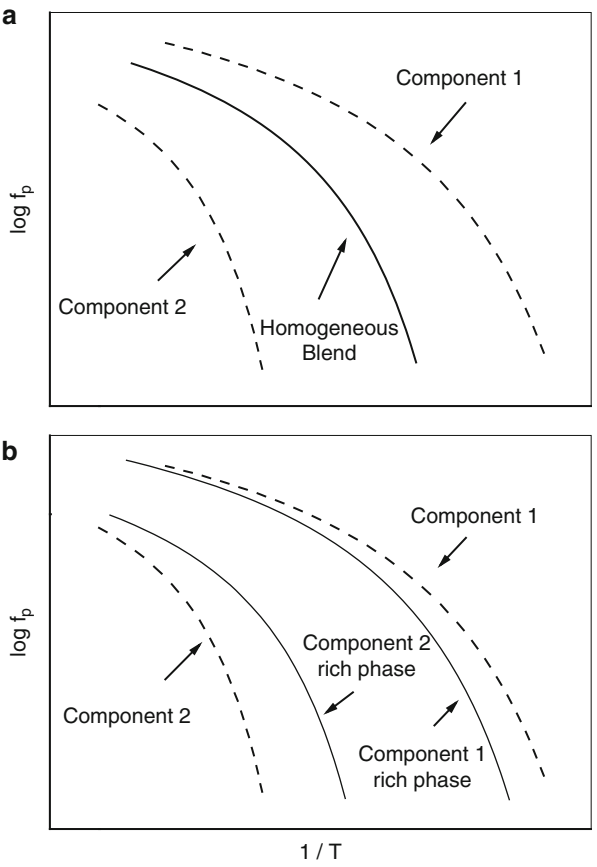

Fig. 12.14 Schematic representation (relaxation map) of the temperature dependence of the rate of the α-relaxation for a binary polymeric blend: (**a**) theoretical expectation for a molecular miscible blend. (**b**) A blend with a partial miscibility of the two components

phases (see Fig. 12.14b). Therefore, dielectric spectroscopy is expected to provide valuable information on the local fluctuations of concentrations and on the local miscibility.

Therefore, dielectric spectroscopy can be used to detect and to define criteria of miscibility on a molecular level (Zetsche et al. 1990) by studying the dynamic glass transition. Moreover, both components of a blend will have different polarities in general. One component can be dielectrically more visible than the other one. In the limiting case one component can be dielectrically invisible (Zetsche et al. 1990). Extending this idea by blending a type-A and a type-B polymer, the overall chain dynamics can be studied only for the polymer of type A employing dielectric spectroscopy. Taking advantage from the fact that the chain dynamics of type-B polymer is dielectrically invisible, one can raise the question how the chain motion of the type-A polymer is influenced by the second component. The normal mode relaxation senses a larger length scale than the segmental one, so information about composition fluctuations on different length scales can be deduced. This was discussed, for instance, for blends of polybutadiene and *cis*-1,4-polyisoprene

(Adachi and Kotaka 1993; Adachi et al. 1995; Poh et al. 1996), polystyrene and *cis*-1,4-polyisoprene (Se et al. 1997), *cis*-1,4-polyisoprene and poly(vinyl ethylene) (PVE) (Hirose et al. 2003), or poly(n-butyl acrylate) and poly(propylene glycol) (Hayakawa and Adachi 2000a, b).

Concerning the localized β-relaxation, it was found if the interaction of the two components are weak (athermal blends) the effect of blending on this relaxation process is small (see, for instance, Schartel and Wendorff 1995; Pathmanathan et al. 1986; Cendoya et al. 1999; Urakawa et al. 2001; Dionissio et al. 2000). These dielectric results are also in agreement with quasielastic neutron scattering investigations (Arbe et al. 1999) and are probably a consequence of the rather small length scale (localized fluctuations) of motions involved in these processes. This is further discussed also in reference Fischer et al. (1985).

12.4.2 Miscible Polymeric Blends

12.4.2.1 Dynamic Glass Transition: Experimental

There is a considerable large literature body concerning the dielectric relaxation of binary polymer blends especially in the temperature range of the dynamic glass transition (see, for instance, Floudas et al. 2011; Colmenero and Arbe 2007; Zetsche et al. 1990; Adachi et al. 1995; Poh et al. 1996; Se et al. 1997; Hirose et al. 2003; Schartel and Wendorff 1995; Dionissio et al. 2000; Arbe et al. 1999; Wetton et al. 1978; Alexandrovich et al. 1980; Miura et al. 2001; Rellick and Runt 1986a, b, 1988; Angeli and Runt 1990; Alvarez et al. 1997; Hoffman et al. 2002; Cangialosi et al. 2005, 2006; Alegria et al. 2002; Leroy et al. 2002, 2003; Lorthioir et al. 2003; Schwartz et al. 2007a, b; Jin et al. 2004; Ngai and Roland 2004; Watanabe et al. 1991, 1996; Urakawa et al. 1993a, b, 2006; Katana et al. 1995, 1993, 1992; Zetsche and Fischer 1994; Karatasos et al. 1998; Sy and Mijovic 2000; Roland et al. 2006; Zhang et al. 2005; Mpoukouvalas et al. 2005; Pathak et al. 1999; Krygier et al. 2005).

Broadening of the Relaxation Spectrum

It is known for a long time (Wetton et al. 1978) that the relaxation function measured for a miscible blend is considerably broadened compared to the spectra of the pure polymers (Colmenero and Arbe 2007). To be more precise the broadening is more or less symmetric. As an example this is shown for a miscible blend of polystyrene (PS) and poly(vinyl methylether) (PVME) in Fig. 12.15 (Colmenero and Arbe 2007; Katana et al. 1992; Zetsche and Fischer 1994). Compared to PVME the dipole moment of PS is weak, and therefore, the contribution of PS to the dielectric loss of the blend is negligible. In other words the fluctuations of PVME are selectively monitored by dielectric spectroscopy, whereas the fluctuations of the PS segments are dielectrically invisible. For the blend (see Fig. 12.15b), the loss peak is much broader than that for the single component PVME (see Fig. 12.15a). Moreover, the loss peak narrows as temperature increases. For the PVME/PS blend system, it was proven by a combination

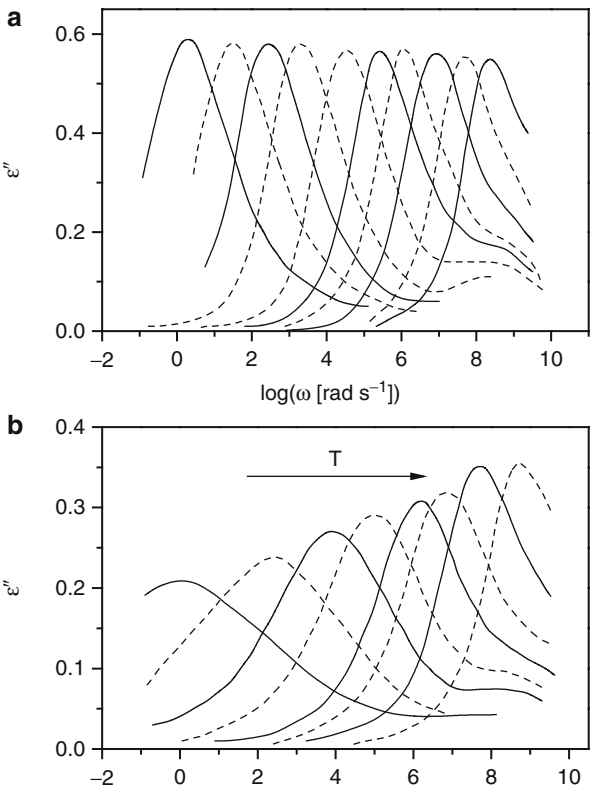

Fig. 12.15 Dielectric loss for the PVME/PS blend at a composition of 65 % PVME/35 % PS. (**a**) Dielectric loss versus frequency for pure PVME: (T = 253 K, 258 K, 263 K, 268 K, 278 K, 288 K, 298 K, 308 K, 328 K, 348 K). (**b**) Dielectric loss versus frequency for PVME/PS blend: (T = 263 K, 273 K, 283 K, 293 K, 308 K, 318 K, 338 K, 368 K) (Data were taken from reference Cendoya et al. (1999))

of dielectric, NMR, and quasielastic neutron scattering investigations using deuterated polystyrene that the shape of the relaxation function is similar to that of the corresponding homopolymer at high temperatures (Colmenero and Arbe 2007).

The broadening of the dielectric spectra for miscible polymer blends is not only observed for the PS/PVME system. This further demonstrated by Fig. 12.16 where the normalized dielectric loss is plotted for a blend poly(ethylene-co-vinyl acetate) (EVA70, 70 % vinyl acetate) with poly(vinyl chloride) (PVC). With increasing concentration of PVC in the blend, the loss peak systematically broadens in comparison to that of both components (Rellick and Runt 1988).

The broadening of the dielectric spectra has to be considered as an intrinsic feature of the dielectric properties of miscible blends. Moreover, the broadening of the α-relaxation increases with the difference of the glass transition temperatures.

A phenomenological treatment is most simple if one component is dielectrically more or less invisible as it is the case for polystyrene. In this case the broadening of the loss peak can be described by a distribution function $\widetilde{c}$ in the sense of Eq. 12.27:

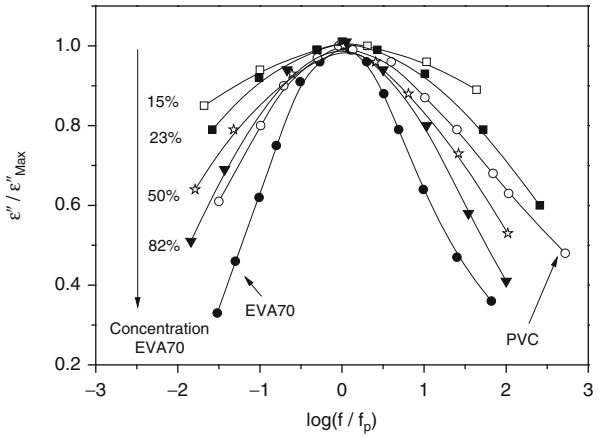

Fig. 12.16 Normalized dielectric loss versus normalized frequency for the blend system EVA70/PVC. Parameter is the concentration of EVA70 in the blend as indicated. *Lines* are guides for the eyes (Data were taken from reference Rellick and Runt (1986b))

$$\varepsilon''_{\text{Blend}}(\omega) = \int_0^\infty \tilde{c}(\tau)\, \varepsilon''_{\text{Vis}}(\omega\tau)\, d\tau. \tag{12.53}$$

$\varepsilon''_{\text{Vis}}(\omega)$ is the relaxation function of the dielectrically visible component of the blend. Clearly $\tilde{c}$ should be related to the molecular structure of the miscible blend. Equation 12.53 is derived under the assumption that the "live time" of $\tilde{c}$ is much longer than the longest relaxation time for the α-relaxation. Often $\tilde{c}$ is assigned on a molecular level to temperature-driven composition fluctuations (Katana et al. 1995; Zetsche and Fischer 1994) which will be discussed in detail later.

Adachi et al. (Hayakawa and Adachi 2000b) suggest the following formula for the complex dielectric function of a miscible blend:

$$\varepsilon^*_{\text{Blend}}(\omega) = \Phi_1 \varepsilon^*_1 \left(\frac{\zeta_{\text{Blend}}}{\zeta_1}\omega\right) + \Phi_2 \varepsilon^*_2 \left(\frac{\zeta_{\text{Blend}}}{\zeta_2}\omega\right), \tag{12.54}$$

where ε^*_i are the complex dielectric function of pure components and ζ_i the corresponding monomeric friction coefficients (for definition see Ferry 1980; Sperling 1986; Strobl 1996). This formula is firstly based on the idea that the dipole moment of the mixture is a weighted sum of the dipole moments of each component. Secondly, the segmental mobility in the blend can be described by a common friction coefficient ζ_{Blend}. According to this assumption the segmental relaxation time τ_i for the pure component i has to be changed to $\tau_i \frac{\zeta_{\text{Blend}}}{\zeta_i}$. For the friction coefficient of the blend ζ_{Blend},

$$\ln \zeta_{\text{Blend}} = \Phi_1 \ln \zeta_1 + \Phi_2 \ln \zeta_2 + k\Phi_1\Phi_2 \tag{12.55}$$

was suggested. k is a parameter which characterizes the interaction between the two components. Please note that the k parameter can be different from the Flory/Huggins interaction parameter. This model can also qualitatively describe experimental results (Hayakawa and Adachi 2000a, b).

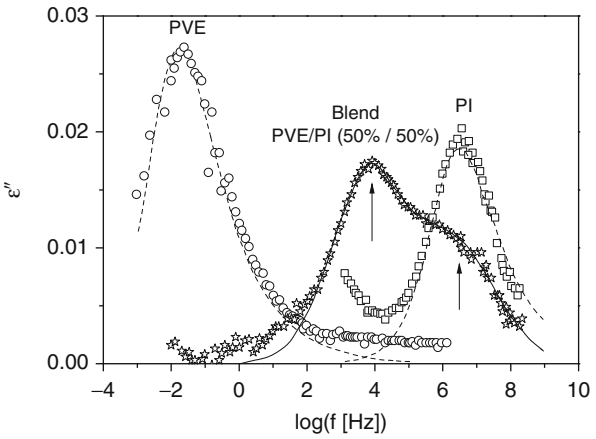

Fig. 12.17 Dielectric loss versus frequency at 270 K for the PVE/PI blend at a composition of 50 % PVE/50 % PI. *Circles*, pure PVE; *squares*, pure PI; *stars*, blend PVE/PI. *Lines* are estimated contributions of the dynamic glass transition (Data were taken from reference Arbe et al. (1999))

Dynamic Heterogeneity

For the simple theoretical approach outlined in Fig. 12.14a, one should expect that for a blend which is fully miscible on a molecular level, only a single relaxation process with a single average relaxation rate (or time) should be observed. In other words this would correspond to a single average $<T_g>$ measured by DSC. Figure 12.17 gives the dielectric spectra of poly(vinyl ether) (PVE) and *cis*-1,4-polyisoprene (PI) together with results for the blend PVE/PI (50 %/50 %) according to reference Arbe et al. (1999). For the PVE/PI system both components are dielectrically visible. For the blend a two peak structure is observed. It is worth to point out that this double peak structure is observed independently of the already discussed broadening of the α-relaxation peak. That was proven by quasielastic neutron scattering investigations where both components of the blend were selectively deuterated (Hoffman et al. 2000). This effect observed for a variety of miscible binary polymer blends and is called "dynamic heterogeneity."

Further evidence for the dynamical heterogeneity in miscible polymer blend was provided by a combination of DSC and TSC measurements. While DSC is sensitive to the molecular dynamics of the whole blend, TSC monitors selectively the molecular fluctuations of the polar component. Figure 12.18 compares the temperature dependence of specific heat capacity with that of the depolarization current for the blend system PVME/PS (Leroy et al. 2002). For the polar component PVME, the peak in the TSC curve collapses with the midpoint of the steplike change of the specific heat capacity usually taken as thermal glass transition temperature. This indicates that both methods sense the same process which is the molecular fluctuation of PVME segments responsible for the glass transition. For the blend a broad DSC trace is observed but with a single step in the specific heat capacity indicating miscibility. In difference to the thermal data, the TSC peak is observed at essential lower temperatures. This means the effective ("local") $T_{g,eff}$ due to the polar PVME segments is observed at much lower temperatures than the overall T_g ($<T_g>$) of the blend and proves that an $T_{g,eff}$ different from $<T_g>$ exists (Leroy et al. 2002).

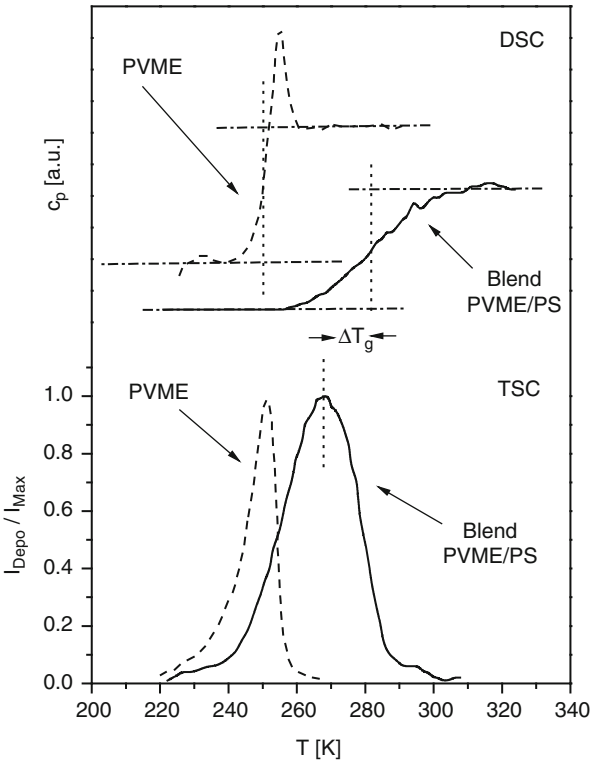

Fig. 12.18 Comparison of DSC and TSC measurements for pure PVME (*dashed lines*) and a PVME/PS (*solid lines*) at a composition of 50 % PVME/50 % PS. *Dotted vertical lines* indicate the glass transition temperatures (Data were taken from reference Leroy et al. (2002))

In reference Leroy et al. (2002), this was investigated for three different blend systems. Also Lodge and coworkers evidenced the existence of two different glass transitions in miscible blends by DSC measurements alone (Lodge et al. 2006) or by a combination of DSC and TSC investigations (Herrera et al. 2005). A similar conclusion was provided by a combination of dielectric spectroscopy with adiabatic calorimetry (Sakaguchi et al. 2005) or employing temperature-modulated DSC (Miwa et al. 2005). Results provided in reference Schwartz et al. 2007b can be discussed in the same direction. In conclusion, besides the broadening of the relaxation spectrum, the dynamic heterogeneity must be considered as the second main feature of the (dielectric) properties of miscible blends.

Kirkwood/Fröhlich Correlation Factor

In Sect. 12.2.2.1 the Kirkwood/Fröhlich correlation factor g as a measure of static correlations between dipoles is introduced and discussed (see Eq. 12.14). It seems to be an interesting question in which way g is changed in miscible blends. Data are provided, for instance, in references Wetton et al. (1978), Alexandrovich et al. (1980), and Malik and Prud'homme (1984) using Eq. 12.14. As a result it was observed that the g parameter is only weakly affected by blending

(Alexandrovich et al. 1980; Rellick and Runt 1986b) in the whole considered concentration range. This means the conformation of segments was not significantly changed in the blend. Runt et al. (Rellick and Runt 1986b) derived an equation to assess the effect on blending on the g-factor relative to the unblended state:

$$g_{Blend} = 9\varepsilon_0 k_B T \frac{\frac{\Delta\varepsilon\,(2\varepsilon_s+\varepsilon_\infty)}{n\,\varepsilon_S}}{g_1 n_1 \mu_1^2 \left(\varepsilon_\infty^1 + 2\right)^2 + g_2 n_2 \mu_2^2 \left(\varepsilon_\infty^2 + 2\right)^2}, \tag{12.56}$$

where subscript i indicates the component, n the overall dipole density in the blend, and n_i the mole fraction of the component i in the blend. The numerator is the effective squared dipole moment in the blend where the denominator was obtained by a linear combination of the dielectric properties of the blend. Then g_{Blend} is a measure of the polarization of the blend with respect to an unblended environment (Rellick and Runt 1986b; Angeli and Runt 1989).

12.4.2.2 Dynamic Glass Transition: Theoretical Models

Most researchers will agree that the molecular fluctuations of a segment i of a polymer "A" in binary blend are controlled by the local composition ϕ_i in some volume around that segment. This local concentration which is different from the macroscopic blend composition will give rise to a relaxation time τ_i which is different from the mean relaxation time. In general we have a distribution of different environments having different compositions ϕ_i which will lead to a distribution of relaxation times and hence results in a broadening in the loss curve. A further consequence of this distribution at a segment i is a distribution of local T_g.

One approach to model this effect is based on the coupling scheme of Ngai et al. (Roland and Ngai 1991, 1992a, b). In this scheme a so-called coupling parameter determines the shape of the relaxation function. In its application to blends, the local concentrations ϕ_i lead to a distribution of the coupling parameter which will consequently cause a broadening of the relaxation function.

Besides the coupling model two other groups of model have been developed during the last 15 years: the model of "temperature-driven composition fluctuations" at the one side and the idea of "self-concentration" on the other side.

Temperature-Driven Concentration Fluctuations (TCF)

The idea of temperature-driven concentration or composition fluctuation traces back to Karazs et al. (Wetton et al. 1978). One of the first models was developed by Fischer et al. (Katana et al. 1995; Zetsche and Fischer 1994). This work was further extended in several directions by Kumar and Colby et al. (Salaniwal et al. 2002; Kamath et al. 2003a, b, 1999; Kumar et al. 1996, 1999; Kant et al. 2003).

The temperature-driven concentration fluctuation approach is based on the following assumptions (see Fig. 12.19):

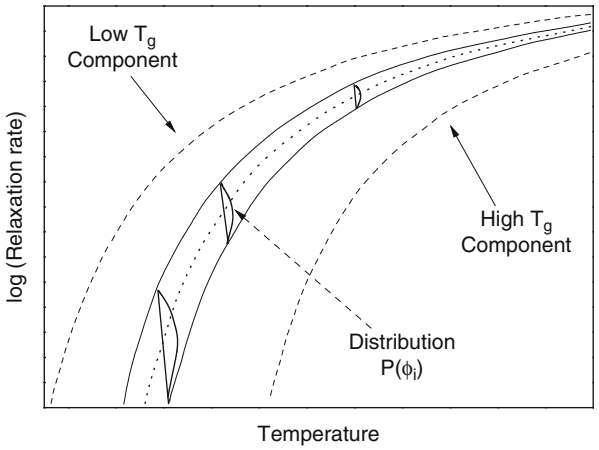

Fig. 12.19 Scheme of the temperature-driven concentration fluctuation approach to binary miscible blends

1. The sample is divided into i subcells of the volume V having a composition ϕ_i and thus a local glass transition temperature $T_g^i(\phi_i)$.
2. A distribution $P(\phi_i)$ of the composition ϕ_i is introduced. This will lead to a distribution of relaxation times and also a distribution of the local glass transition temperatures $T_g^i(\phi_i)$. In the approach by Fischer et al. (Katana et al. 1995; Zetsche and Fischer 1994), $P(\phi_i)$ was assumed to be Gaussian with a variance $<(\delta\phi)^2>$. In this model $<(\delta\phi)^2>$ is the only adjustable parameter. Extending this model non-Gaussian distributions have been also discussed, for instance, by Kumar (Kumar et al. 1996).
3. The system is incompressible which means that density fluctuations do not exist.
4. The lifetime of the composition fluctuations is much longer than the longest relaxation time for the α-relaxation.

One open point in the discussion untill now is the size of the volume V. Usually it is assumed that V is related to the cooperatively rearranging region (CRR, $V \sim V_{CRR}$, see discussions above) characteristic for the glass transition. It can be estimated taking advantage from the fact that for a Gaussian distribution $P(\phi_i)$ V should be inversely proportional to $< (\delta\phi)^2 >$ ($V \sim < (\delta\phi)^2 >^{-1}$). A quantification can be done by assuming the CRR to be spherical and relating $<(\delta\phi)^2>$ to the static structure factor S(Q) in the same way as it was proposed by Ruland for density fluctuations (Ruland 1957). This approach is based on the random phase approximation (de Gennes 1979). In reference Katana et al. (1995), a comparison is made between the values estimated from that approach and the V_{CRR} calculated from the fluctuation approach by Donth (see Eq. 12.49). The data are in the same order of magnitude but do not agree quantitatively.

The TCF models are able to describe the broadening of the relaxation function as temperature approaches the average glass transition temperature $<T_g>$. It can be also seen from Fig. 12.19 that the extra-broadening due to blending decreases with increasing temperature. The main problem of that approach is the fact that these

models have no explanation for the heterogeneous behavior. Moreover, the estimated length scales for glass transition $\xi \sim V_{CRR}^{1/3}$ grow too strongly as temperature decreases towards $<T_g>$ and can become larger than 10–20 nm. This is much too large than expected for the glass transition. A more detailed discussion can be found, for instance, in reference Colmenero and Arbe (2007).

Self-Concentration Models (SC)

The idea of self-concentration in polymer blends was mainly developed by Lodge and McLeish (2000) based also on earlier works of Kornfield et al. (Chung et al. 1994a, b). For reviews in relation to dielectric spectroscopy, see, for instance, references Colmenero and Arbe (2007) and Maranas (2007). The basic idea is that due to chain connectivity the average composition in local environment around any selected segment is enriched in the same kind of segments (correlation hole effect). In consequence this will lead to different average relaxation times for the segment of the two components in the blend and hence each component will sense its own glass transition temperature which is of course composition dependent. For this reason the self-concentration can account for the heterogeneity effects in the dynamic of polymer blends.

In the formulation of Lodge and McLeish (2000) (LM model) for a binary blend with the components i (i = 1,2), the effective concentration is

$$\phi_{eff}^{i} = \phi_{self}^{i} + \left(1 - \phi_{self}^{i}\right) < \phi > , \tag{12.57}$$

where $<\phi>$ is the overall macroscopic composition of the blend. Because of the chain connectivity, the relevant intramolecular length scale to estimate the self-concentration is the Kuhn segment length l_k (Strobl 1996) which is only weakly temperature dependent. The self-concentration can be estimated from the volume fraction due to monomers in a volume spanned by the Kuhn length ($V_k \sim {l_k}^3$) as

$$\phi_{self} = \frac{C_\infty M_0}{k \rho N_A V_K}, \tag{12.58}$$

where C_∞ is the characteristic ratio, ρ density, M_0 the molar mass of the repeating unit, N_A Avogadro number, and k counts the number of backbone per repeating unit. The effective glass transition temperature is defined as

$$T_{g,\,eff}^{i} = \; < T_g > \left(\phi = \phi_{eff}^{i}\right). \tag{12.59}$$

Besides the self-concentration the Lodge and McLeish model assumes further that the composition of the volume V is similar to the macroscopic one. Basically this means that one distribution of relaxation times (or T_g) is involved. The LM model treats in contradiction to the TCF approach only mean values. But it is interesting to note that also self-concentration effects decreases with increasing temperature.

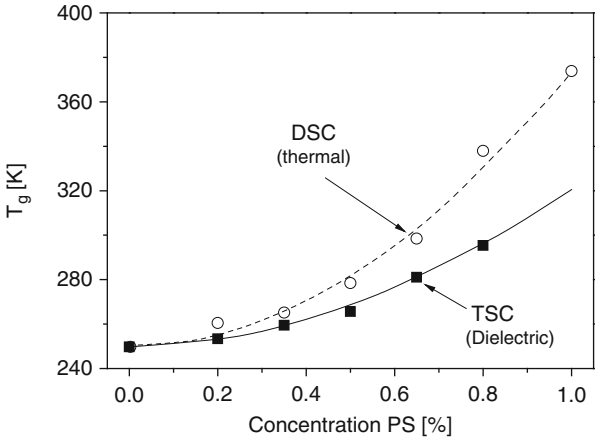

Fig. 12.20 Glass transition temperatures for the blend system PVME/PS versus the concentration of PS. The *open spheres* are data measured by DSC indicating the macroscopic T_g of the sample. The *solid squares* are data measured by TSC for the dielectrically visible component PVME. The *dashed line* is a fit of the Brekner equation to the DCS data. The *solid line* corresponds to the prediction of the LM model according to Eq. 12.61 (Data were taken from reference Rellick and Runt (1986))

In Fig. 12.20 the DSC and TSC data for the blend system PVME/PS discussed in Fig. 12.18 are analyzed in the framework of the LM model (for details see reference Leroy et al. 2002). The glass transition temperature of the blend measured by DSC is described by the Brekner formula (Brekner et al. 1988):

$$T_g(\phi^2) = T_g^1 + \left(T_g^2 - T_g^1\right)\left[(1+K_1)\phi^2 - (K_1+K_2)\left(\phi^2\right)^2 + K_2\left(\phi^2\right)^3\right]. \tag{12.60}$$

ϕ^2 is the blend concentration of the polymer with the higher T_g value, and T_g^i ($i = 1,2$) are the glass transition temperatures of the pure polymers. K_1 and K_2 are fitting constants. By combining Eqs. 12.57, 12.59, and 12.60 according to Lodge and McLeish (2000), the glass transition temperature for the individual components can be estimated. For the component with the higher T_g^2, one obtains

$$T_{g,\mathrm{eff}}^2(\phi^2) = T_g^1 + \left(T_g^2 - T_g^1\right)\left[(1+K_1)\phi_{\mathrm{eff}}^2 - (K_1+K_2)\left(\phi_{\mathrm{eff}}^2\right)^2 + K_2\left(\phi_{\mathrm{eff}}^2\right)^3\right]. \tag{12.61}$$

An analogous equation can be obtained for T_g^1. For details see reference Leroy et al. (2002). Figure 12.20 reveals a remarkably good agreement between the experimental data and the predictions of the LM model.

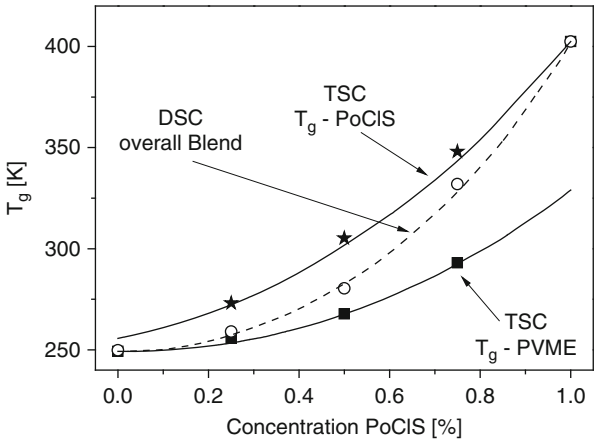

Fig. 12.21 Glass transition temperatures for the blend system PVME/PoClS versus the concentration of PoClS. The *open spheres* are data measured by DSC indicating the macroscopic T_g of the sample. The *solid squares* are data measured by TSC for PVME, whereas the stars are TSC data measured for PoClS. The *dashed line* is a fit of the Brekner equation to the DCS data. The *solid line* corresponds to the prediction of the LM model for both the low and the high glass transition temperature component (Data were taken from reference Leroy et al. (2002))

The same approach was also applied by Colmenero et al. to poly (vinyl methylether) blended with poly(o-chlorostyrene) (PoClS) (Leroy et al. 2002). The difference to the PVME/PS is that in the case of PVME/PoClS system, both components are polar and therefore dielectrically visible. Figure 12.21 shows the results for this system also obtained by a combination of DSC and TSC investigations. Again a good agreement with the LM model is obtained.

The self-concentration model by Lodge and McLeish can be also employed to describe the relaxation map of a miscible blend system. In reference Mpoukouvalas and Floudas (2008), Floudas et al. report dielectric data for the miscible blend poly (methyl methacrylate) (PMMA) and poly(ethylene oxide) (PEO) (see Fig. 12.22). As expected, with increasing concentration of PEO the relaxation rates shifts to lower temperatures. The data can be modeled by assuming the Vogel temperature T_0 in the VFT equation (see Eq. 12.45) to be dependent on the effective concentration according to Eq. 12.57:

$$-\log f_p^i = \log\tau^i(\phi_{eff}, T) = \log\tau_\infty^i + \frac{A^i}{T - T_0^i(\phi_{eff})}, \tag{12.62}$$

where A^i and τ_∞^i are the VFT parameters for the two components. In this approach only the Vogel temperature depends on composition according to

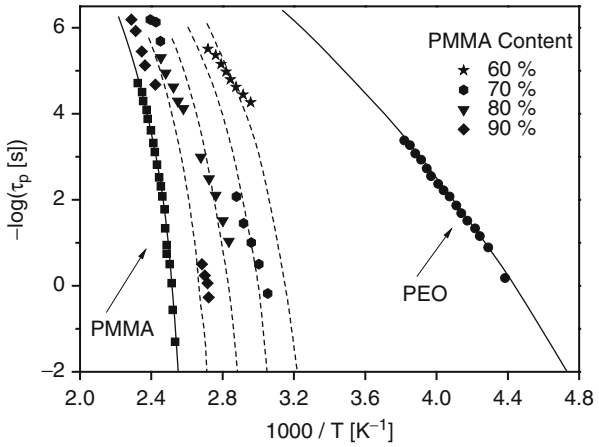

Fig. 12.22 Temperature dependence of the relaxation times of the segmental dynamics (α-relaxation) for the blend system PMMA/PEO at the indicated concentrations: *solid squares*, PMMA; *solid circles*, PEO. The *solid lines* correspond to fits of the VFT equation to the data of the pure polymers. The *dashed lines* are due to fits of the LM model with the Kuhn lengths for PMMA as adjustable parameter ($l_k = 1.62$ nm, theoretical value 1.38 nm) (Data were taken from reference Mpoukouvalas and Floudas (2008). The concentration dependence of the whole blend was described by the Fox/Flory equations. For details see also reference Mpoukouvalas and Floudas (2008))

$$T_0^i(\phi_{eff}) = T_0^i + \left[T_g^i(\phi_{eff}) - T_g^i\right], \tag{12.63}$$

where T_0^i are the Vogel temperatures of the pure polymers and $T_0^i(\phi_{eff})$ the value of the Vogel temperature for the polymer i in the blend. As Fig. 12.22 shows this approach can reasonably describe the segmental dynamics of PMMA in the blend PMMA/PEO under the condition that l_k is adjusted to 1.62 nm which is larger than the theoretical value of 1.38 nm (Mpoukouvalas and Floudas 2008). This means, the self-concentration approach covers some intrinsic features of the molecular dynamics in polymer blends. A better agreement can be obtained by adjusting l_k for each blend composition.

As discussed above the self-concentration idea is able to describe one essential experimental fact of the molecular dynamics of polymer blends, the dynamic heterogeneity. But nevertheless there are some strong problems of this approach which are discussed in detail in reference Colmenero and Arbe (2007). Here only the main arguments are summarized:

1. The most important drawback of the self-concentration approach is the fact that the model cannot describe the broadening of the relaxation function induced by blending. Attempts to combine the self-concentration idea with that of temperature-driven composition fluctuations are discussed, for instance, in reference Leroy et al. (2003) and more recently in Shenogin et al. (2007).

2. In the original version of the LM model, ϕ^{i}_{self} is assumed to be independent of temperature that is found in some cases. But in other cases the data can be only described allowing ϕ^{i}_{self} to be temperature dependent. This concerns also the relevant length scale ξ, which is in the LM approach the Kuhn length known to be only weakly temperature dependent. Experimentally it was motivated that ξ could be dependent on temperature (Colmenero and Arbe 2007) as well as on pressure (Mpoukouvalas and Floudas 2008). This length scale can be also dependent on the composition and the components (Lutz et al. 2005; He et al. 2003).

Combination of the Self-Concentration Approach with the Adam/Gibbs Theory

In the framework of the Adam and Gibbs theory, the temperature-dependent size of a CRR is related to the spatial extent of cooperative segmental fluctuations at the dynamic glass transition. For polymer blends the effect of chain connectivity depends on temperature and can be less or more pronounced. Therefore, the assumption of a temperature-dependent CRR has some consequences for the relevant length scale responsible for glassy dynamics. Recently the approach of self-concentration was combined with the theory of Adam and Gibbs to the glass transition (Cangialosi et al. 2005). Two essential assumptions are made. Firstly, the systems should behave athermal – this means that thermodynamic quantities are additive according to the composition. Secondly, both the configurational entropy S_C and the constant C (see Eq. 12.47) are assumed to be depend on the effective concentration according to Eq. 12.57:

$$S_C^{1/Blend} = \phi_{eff}^1 S_C^1 + \left(1 - \phi_{eff}^1\right) S_C^2; \quad C^{1/Blend} = \phi_{eff}^1 C^1 + \left(1 - \phi_{eff}^1\right) C^2. \tag{12.64}$$

It is worth to note that $S_C^{1/Blend}$ and $C^{1/Blend}$ are related to a region (radius r_C) centered around a segment of the polymer 1 relevant to the dynamics of the α-relaxation. (Similar equations can be written down for polymer 2).

Depending on the value of r_C with respect to the Kuhn length l_k, the self-concentration can be estimated using simple geometrical arguments to

$$\phi_{self} = \frac{l_k l_P}{2\pi r_C^2} \quad \text{for } r_C < l_k \quad \text{and} \quad \phi_{self} = \frac{3 l_p}{2\pi r_C} \quad \text{for } r_C > l_k. \tag{12.65}$$

l_P is a packing density. In the Adam/Gibbs approach, the number of correlated segments is proportional to ${S_C}^{-1}$. Therefore, r_C can be related to the configurational entropy by $r_C = \alpha\, S_C^{-1/3}$where α is a constant which can be obtained in principle by fitting experimental data. With that the self-concentration can be expressed by the configurational entropy:

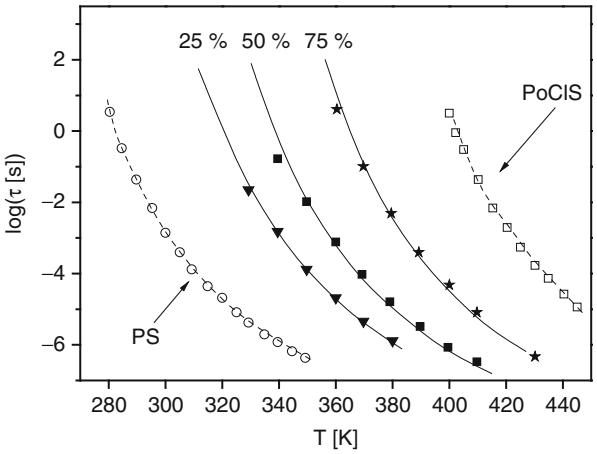

Fig. 12.23 Relaxation time versus temperature for the blend system PS/PoClS: *open circles*, pure PS (molecular weight 700 g/mol); *triangles*, 25 % PoClS; *squares*, 50 % PoClS; *stars*, 75 % PoClS; *open squares*, pure PoClS. The *solid lines* are fits of the combined Adam/Gibbs – self-concentration approach as described in the text. The *dashed lines* are fits of the Adam and Gibbs model to the data of the pure components. For details see reference (Data were taken from reference Cangialosi et al. (2005))

$$\phi_{self} = \frac{l_k\, l_P}{2\pi\,\alpha^2} S_C^{2/3} \quad \text{for } r_C < l_k \quad \text{and} \quad \phi_{self} = \frac{3 l_p}{2\pi\,\alpha} S_C^{1/3} \text{ for } r_C > l_k. \tag{12.66}$$

To apply this approach to experimental data, several further assumptions have to be made: (1) the prefactor for the temperature dependence of the relaxation times or rates of the blends is similar to that of the pure components, (2) the configurational entropy S_C is expressed by the excess entropy $S_C \sim S_{Ex} = S^{Melt} - S^{Crys}$ where Eq. 12.64 applies also for S_{Ex}, and (3) the contribution of the vibrations to the excess entropy is similar for the two components in the blend. Under these assumptions the temperature dependence of the relaxation times for the blends can be described for several systems. This is demonstrated in Fig. 12.23 for the blend system PS/PoClS (Cangialosi et al. 2005).

This approach was further extended in reference Cangialosi et al. (2007) to estimate the absolute size of a CRR. Therefore, the parameter α has to be obtained quantitatively. As a result for a variety of polymers, the size of a CRR was found to be between 1 nm and 3 nm at the glass transition. These numbers are in agreement with the fluctuation approach by Donth (Donth et al. 2001b; Hempel et al. 2000; Beiner et al. 1998; Kahle et al. 1997) as well as with more recent theories using approximations of higher order correlation functions (Berthier et al. 2005; Dalle-Ferrier et al. 2007).

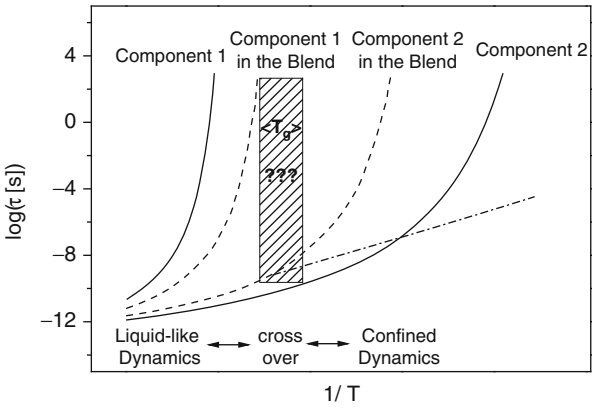

Fig. 12.24 Scheme of the dynamics of dynamic asymmetric blends

12.4.2.3 Dynamically Asymmetric Polymer Blends: Confinement Effects

Besides the dynamic heterogeneity discussed above, binary miscible polymer blends can be considered as dynamically asymmetric if the two components have a large difference in the glass transition temperatures. Usually the dynamic asymmetry is defined by $\Delta = \tau^{1/\mathrm{Blend}}/\tau^{2/\mathrm{Blend}}$ where $\tau^{\mathrm{i/Blend}}$ is the relaxation time of the component i in the blend and 1 is the polymer with the higher glass transition temperature (Colmenero and Arbe 2007). It becomes clear from Fig. 12.19 that the dynamic asymmetry decreases with increasing temperature.

Figure 12.24 gives schematically the relaxation map for the α-relaxation of a polymer blend where the two components have a large difference in their glass transition temperatures. The solid lines indicate the behavior of the pure polymers where the dashed lines correspond to the heterogeneous dynamics of miscible blends which can be estimated by the LM model. It becomes clear from Fig. 12.24 that the dynamic asymmetry Δ is small and both blend components behave as expected. With decreasing temperature Δ increases strongly and the segmental dynamics of the polymer 1 (component in the blend with the higher T_g) slows more and more down. This will have some implications onto the dynamics of the component 2 having a lower T_g. These segments have to fluctuate in a kind of more and more frozen environment built by the segments of the component 1 which will act as a rigid confinement. As it is known for low-molecular-weight glass formers and polymers confined to nanoporous glasses (Zorn et al. 2002; Schönhals et al. 2005), polymer segments embed between liquid crystalline structures (Turky et al. 2012), as well as water intercalated in the intergalleries of clays (Swenson et al. 2001) or in pores (Gallo 2000), such a confinement will lead to a crossover from a VFT behavior at high-temperature behavior to an Arrhenius-like dependence at low temperatures because of the fact that the molecular fluctuations become localized due to the confinement relative to that what is expected for the confined state. According to Fig. 12.24 this is also expected for dynamically asymmetric blends.

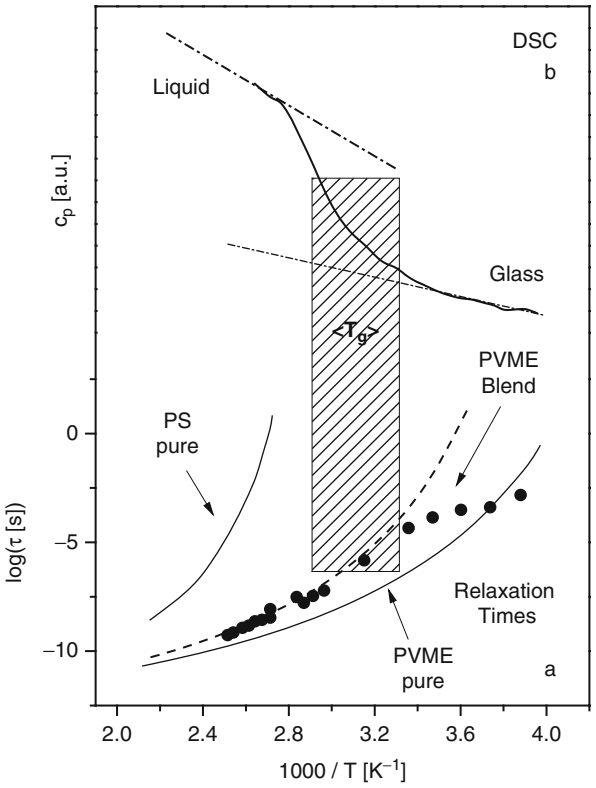

Fig. 12.25 Result for the dynamic asymmetric blend PS/PVME at a composition 80 %/20 %. *Lower panel*: *solid spheres*, dielectric data; *dashed line*, temperature dependence of the relaxation times expected for PVME in the blend; *solid lines* indicate the temperature dependence of the relaxation times for the pure components. *Upper panel*: temperature dependence of the heat capacity measured by DSC (All data were taken from reference Cendoya et al. (1999))

Figure 12.25a shows dielectric results for the blend system PVME (T_g = 249 K)/PS (T_g = 373 K) at a composition of 20 % PVME/80 % PS which is rich in the component with the higher T_g PS (see reference Cendoya et al. 1999). Due to the low dipole moment of PS, it is dielectrically invisible in the blend and only the segmental dynamics of the low T_g component PVME is dielectrically monitored. It is evident from Fig. 12.25a that the temperature dependence of the PVME segments in the blend is curved and follows the VFT equation. In the broad range of the glass transition of the whole blend measured by DSC (see Fig. 12.25b), this VFT temperature dependence crosses over to an Arrhenius-like behavior which is fully developed at even lower temperatures. Because of the fact that the blend is rich in PS, the DSC measurement monitors mainly the glass transition of polystyrene. This fact implies that the crossover in the temperature dependence of PVME is really due to the freezing of the PS segments. In the same temperature range also characteristic deviations in the temperature dependence of the forward scattering intensity S(Q→0) obtained from small angle neutron scattering from the predictions of the random phase approximation are observed for the same system (Koizumi 2004). These deviations are consistent with the formation of a gel-like structure due to the freezing of the PS segments.

Similar results have been also reported by Adachi et al. (Urakawa et al. 2002) for PVME/PS, for the blend PMMA/PEO (Maranas 2007), or for blends of PVDF/PMMA (Sy and Mijovic 2000). Besides dielectric spectroscopy quasielastic neutron scattering is found to be quite useful to investigate the molecular dynamics of dynamic asymmetric polymer blends because spatial information is provided by this technique (see, for instance, Tyagi et al. 2006, 2007). For a more detailed discussion, the reader is referred to the literature (Colmenero and Arbe 2007).

Besides of the segmental dynamics also the chain dynamics in blends is affected by the dynamical asymmetry (Brodeck et al. 2010). Recently a generalized Langevin approach was presented to calculate the chain (Rouse dynamics) for dynamically asymmetric blends (Colmenero 2013). A further discussion is beyond the scope of this chapter.

12.4.2.4 Dielectric Relaxation of Blends Under Pressure

Besides temperature pressure is an important quantity. Moreover, from the applicative point of view, pressure has a direct implication in processing. From the point of basic research, the properties and the thermodynamics of polymer blends are often discussed assuming incompressibility (properties are unaffected of pressure) like in the random phase approximation (de Gennes 1979; Binder 1994) or in the approach of temperature-driven concentration fluctuations (Katana et al. 1995). The effect of pressure on the dielectric properties of blends has been intensively discussed by Floudas et al. (Floudas et al. 2011; Floudas 2003) and is also reviewed in reference Roland et al. (2005). On the one hand as a general result, the assumption of incompressibility seems to be in contradiction to the results obtained by dielectric spectroscopy under pressure (Floudas et al. 2011) as it was also found by other methods in reference Beiner et al. (1998a). Moreover, pressure can increase or decrease miscibility. But one has also to consider that the number of dielectric relaxation studies under pressure is quite limited and different (partly contradictory) results have been found (see discussion in reference Roland et al. 2005). From the experimental point of view, this indicates that the influence of pressure on the molecular dynamics is complex and that more experimental studies should be carried out. Theoretical approaches have been pioneered by Rabeony et al. (Rabeony et al. 1998), by Kumar (Kumar 2000), and by Lipson et al. (lattice-based equation of state) (Lipson et al. 2003, 1998; Tambasco et al. 2006). Recently Colmenero et al. (Schwartz et al. 2007) combined the approach of Adam and Gibbs with the idea of self-concentration as described above by considering also pressure. For the PVME/PS blend system, this approach can describe the temperature dependence of the dielectric relaxation times measured under the different pressures (Schwartz et al. 2007).

12.4.3 Immiscible Blends

Immiscible blends are inhomogeneous systems. For dielectric spectroscopy this fact – like for semicrystalline polymers – has several implications: Firstly,

appropriate mixing rules for the dielectric permittivity have to be applied. For a completely phase-separated structure and if the two components having approximately the same dipole moment in the most simplest case, one can write for the dielectric function of the blend to

$$\varepsilon^*_{\text{Blend}}(\omega) = \Phi_1 \varepsilon_i^*(\omega) + \Phi_2 \varepsilon_2^*(\omega). \tag{12.67}$$

However, in most cases a limited miscibility (depending on N_i and κ) (see Eq. 12.52) is observed leading to two phases enriched in one component which can be described by a concentration C_i. In principle the concepts developed in Sect. 12.4.2 can be employed to model the dielectric properties of each phase. In principle by analyzing the frequency position of the α-relaxation and its dielectric strength, the unknown concentration of each component can be estimated assuming appropriate mixing rules. In practical work this can be difficult. Of special interest is again the case where one component is dielectrically invisible as also discussed in Sect. 12.4.2.

12.4.3.1 Blends with a Semicrystalline Component

Miscible blends where one component of the blend is a semicrystalline polymer and the other one are typical examples for two or more phase systems. In such a system in the amorphous state, both components are miscible, whereas the crystallites appear as a second phase. As a first fact of course, the crystallinity measured, for instance, by DSC or by wide angle X-ray diffraction might be changed by blending. This further implies that the volume fraction of dipoles in the amorphous phase which can become mobile at the glass transition will decrease with increasing crystallinity. This will result in a decrease in the dielectric relaxation strengths. Secondly, the frequency (or temperature) position of the glass transition will shift to lower frequencies (higher temperatures) with increasing crystallinity.

Even for semicrystalline homopolymers it is well-known fact that its morphology cannot be described by a simple two-phase model. A characteristic feature of semicrystalline homopolymers is the so-called rigid amorphous fraction (RAF) (Wunderlich 2003). The RAF is phase which is amorphous in structure but immobilized at the dynamic glass transition of the amorphous phase. Therefore, the steplike change of the heat capacity at the glass transition is smaller than expected. Probably the RAF is located between the crystals and the mobile amorphous regions. Besides DSC the rigid amorphous phase can be also investigated by dielectric spectroscopy (Schlosser and Schönhals 1989; Huo and Cebe 1992a, b, 1993; Cebe and Huo 1994; Kalika and Krishnaswamy 1993). Like for the thermal measurements, the dielectric strength is found to be smaller than expected.

For miscible blends an even more complex behavior is observed as discussed in reference Runt et al. (1991) with regard to interphases. As discussed (Runt et al. 1991) interphases can be consists on the one hand side of segments of the

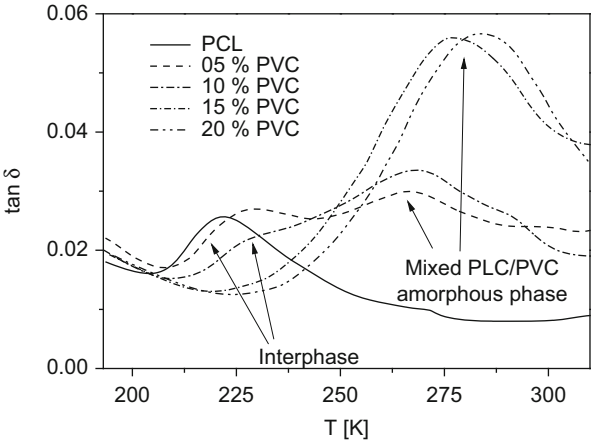

Fig. 12.26 Temperature dependence of dielectric tan δ at a frequency of 2 kHz for melt crystallized PCL/PVC blends at the indicated concentrations (Data were taken from reference Runt et al. (1991))

semicrystalline polymer. Examples for that are blends of poly(vinylidene fluoride) with PMMA or blends of poly(ethylene oxide) also with PMMA. On the other side the interphase can contain segments of both polymers. This is, for instance, the case for blends of poly(butylene terephthalate) with polyarylate or poly(ε-carpolactone) (PLA) mixed with poly(vinyl chloride). As an example for the latter system, Fig. 12.26 depicts the temperature dependence of tan δ for the blend system PLA/PVC at a frequency of 2 kHz. Two relaxation processes are indicated by peaks in tan δ. The process located at lower temperatures is assigned to the discussed interphase where the peak at higher temperatures is related to the segmental fluctuations in the blended PLA/PVC amorphous phase. The interphase process shifts a bit to higher temperatures with increasing concentration of PVC. For concentration greater than 15 % of PVC, the interphase peak disappears.

The discussed situation can become even more complex for cases where a variety of different morphologies have been observed like for blends of polyimides (Hudson et al. 1992; Sauer and Hsiao 1993; Hsiao und Sauer 1993; Li and Kim 1997). This includes the observation of multiple glass transitions (Bristow and Kalika 1997). In this connection one has to note that the existence of a given morphology will depend on the thermal history of a sample like for instance crystallization rates.

12.4.3.2 Interfacial Polarization

Due to the phase-separated structure of immiscible polymer blends including phase boundaries in the corresponding dielectric spectra, Maxwell/Wagner polarization process can be observed especially at low frequencies. As discussed in Sect. 12.2.3.3, the theoretical equations are complex and hard to solve. For certain model systems like inclusion in poly(carbonate filled) with poly(ethylene oxide) (Hayward et al. 1992), it could be shown that for low concentrations the most important quantities are the volume fraction, the geometry of the dispersed phase

(expressed by the shape factor n), and its conductivity as well as the permittivity of the matrix. Also for model systems it was early shown that the shape factor n extracted from the dielectric measurements is in good agreement with the observed morphology using electron microscopy (Steeman et al. 1994). This suggests that from a careful analysis of the dielectric spectra, quantitative conclusions about the morphology of immiscible polymeric blends can be drawn. That also includes the detection of the first stages of a phase-separated structure (Dionisio et al. 1996). Higher concentrations of the dispersed phase were considered, for instance, in reference Banhegyi (1986, 1991).

The most complete theoretical treatment of Maxwell/Wagner polarization process in polymer blends was done by Steeman and coworkers (Steeman and van Turnhout 2003) especially also for higher concentrations of the dispersed phase and multicomponent polymer blends (Steeman et al. 1994; Steeman and Maurer 1990, 1992). Quantitative conclusions about the phase structure of the different systems can be drawn including the modeling also of interfaces. This has also some impact on blend compatibilization by grafted copolymers (Eklind et al. 1997).

12.5 Conclusions

Broadband dielectric spectroscopy is a powerful method to investigate the molecular dynamics of polymeric blend systems. This is particularly due to the fact that an extraordinary broad dynamic range can be covered by this technique in its modern form. Different dielectric active processes can be observed in this extended frequency range like relaxation processes due to the fluctuation of molecular dipole moments, charge transport related to the drift motion of charge carriers, or polarization effects due to the presence of both interfaces and interphases. In this chapter broadband dielectric spectroscopy is discussed in relationship to polymer blends where mainly binary blends are considered. The impact of blending on the different relaxation processes is discussed where special attention is paid on the dynamic glass transition related to segmental dynamics. The main features of miscible binary polymeric blends like broadening of the relaxation function as well as dynamic heterogeneity are discussed in detail. The experimental results are related to theoretical approaches like temperature-driven concentration fluctuations and the self-concentration phenomenon characteristic for chain molecules. Immiscible polymeric blends are briefly reviewed.

12.6 Cross-References

- ▶ Applications of Polymer Blends
- ▶ Mechanical Properties of Polymer Blends
- ▶ Miscible Polymer Blends
- ▶ Morphology of Polymer Blends
- ▶ Thermodynamics of Polymer Blends

List of Important Symbols and Abbreviations

a_T Shift factor
C Concentration
C_1, C_2 Parameters of the WLF equation
D Dielectric displacement
E Electric field strength
E_A, ΔE Activation energy, barrier heights
f Frequency
f_i Relaxation rate at maximal loss, i = β, α, n
$f_{\infty i}$ Preexponential factor, i = β, α, n
Φ_i Volume fraction
ϕ_i Weight fraction
g, g_{intra} Dipolar correlation coefficients
ΔG_M Free energy of mixing
Γ* Reflection coefficient
I, J Current, Current density
k_B Boltzmann constant, $k_B = 1.380662\ 10^{-23}$ J K^{-1}; $k_B = R/N_A$
M, M_W Molecular weight, weight average
N_A Avogadro number ($N_A = 6.022\ 10^{23}$ mol^{-1})
R Gas constant R = 8.314 kJ mol^{-1}
S_C Configurational entropy
ΔS_M Mixing entropy
σ*, σ′, σ″ Complex conductivity, real and imaginary part
T Temperature
T_0 Vogel temperature, ideal glass transition temperature
T_g Glass transition temperature
tan δ Dielectric loss tangent
β, γ Shape parameter of the HN function
ε_0 Permittivity of vacuum ($\varepsilon_0 = 8.854\ 10^{-12}$ As V^{-1} m^{-1})
ε^*, ε′, ε″ Complex dielectric function, real and imaginary part
$\Delta\varepsilon_i$ Dielectric relaxation strength, i = β, α, n,
ζ Monomeric friction coefficient
ξ Correlation length
κ Flory/Huggins interaction parameter
μ Dipole moment
ω Angular frequency (ω = 2*π*f)
τ Relaxation time
τ_{HN} Relaxation time of the HN function
τ_e Time constant for conduction
PEO Poly(ethylene oxide)
PI *Cis*-1,4-Polyisorene
PMMA Poly(methyl methacrylate)
PPG Poly(propylene glycol)
PS Polystyrene

PVAC Poly(vinyl acetate)
PVME Poly(vinyl methylether)
PoClS Poly(o-chlorostyrene)
PVC Poly(vinyl chloride)
U Voltage, different meanings
$\mathbf{Z_S^*(\omega)}$**;** $\mathbf{Z_R^*(\omega)}$ Sample impedance; Reference impedance
$<\ldots>$ Correlation function; Averaged quantities

References

A. Abou Elfadl, R. Kahlau, A. Herrmann, V.N. Novikov, E.A. Rössler, Macromolecules **43**, 3340 (2010)
K. Adachi, T. Kotaka, Prog. Polym. Sci. **18**, 585 (1993)
K. Adachi, T. Wada, T. Kawamoto, T. Kotaka, Macromolecules **28**, 3588 (1995)
G. Adam, J.H. Gibbs, J. Chem. Phys. **43**, 139 (1965)
Agilent Technologies, Agilent PN 4291–1: New technologies for wide impedance range measurements to 1.8 GHz (2000)
A. Alegria, D. Gomez, J. Colmenero, Macromolecules **35**, 2030 (2002)
A. Alegría, O. Mitxelena, J. Colmenero, Macromolecules **39**, 2691 (2006)
P.S. Alexandrovich, F.E. Karasz, W.J. MacKnight, J. Macromol. Sci. Phys. B. **7**, 501 (1980)
F. Alvarez, A. Alegria, J. Colmenero, Macromolecules **30**, 597 (1997)
P.W. Anderson, Science **267**, 1615 (1995)
S.R. Angeli, J. Runt, J. Contemp. Top. Polym. Sci. **6**, 289 (1989)
S.R. Angeli, J. Runt, ACS Polym. Preprints **31**, 286 (1990)
C.A. Angell, Science **267**, 1924 (1995)
A. Arbe, A. Alegria, J. Colmenero, S. Hoffmann, L. Willner, D. Richter, Macromolecules **32**, 7572 (1999)
S. Arrese-Igor, O. Mitxelena, A. Arbe, A. Alegría, J. Colmenero, B. Frick, Phys. Rev. E. **78**, 021801 (2008)
G. Banhegyi, Colloid Polym. Sci. **264**, 1030 (1986)
G. Banhegyi, Polym. Plast. Technol. Eng. **30**, 183 (1991)
J.L. Barton, Verres Refract **20**, 328 (1966)
M. Beiner, H. Huth, Nat. Mater. **2**, 595 (2003)
M. Beiner, G. Fytas, G. Meier, S.K. Kumar, Phys. Rev. Lett. **81**, 594 (1998a)
M. Beiner, S. Kahle, E. Hempel, K. Schröter, E.J. Donth, Macromolecules **31**, 2460 (1998b)
L. Berthier, G. Biroli, J.-P. Bouchaud, L. Cipelletti, D. El Masri, D. L'Hôte, F. Ladieu, M. Pierno, Science **310**, 1797 (2005)
K. Binder, Adv. Polym. Sci. **112**, 181 (1994)
H. Block, Adv. Polym. Sci. **33**, 94 (1979)
A.R. Blythe, *Electrical Properties of Polymers* (Cambridge University Press, Cambridge, 1979)
A. Boersema, J. van Turnhout, M. Wübbenhorst, Macromolecules **31**, 7453 (1998)
R. Böhmer, M. Maglione, P. Lunkenheimer, A. Loidl, J. Appl. Phys. **65**, 901 (1989)
C.J.F. Böttcher, in *Theory of Electric Polarization*. Dielectrics in Static Fields, vol. I (Elsevier, Amsterdam/Oxford/New York, 1973)
M.J. Brekner, H.A. Schneider, H.J. Cantow, Polymer **29**, 78 (1988)
J.F. Bristow, D.S. Kalika, Polymer **38**, 287 (1997)
M. Brodeck, F. Alvarez, A. Moreno, J. Colmenero, D. Richter, Macromolecules **43**, 3036 (2010)
W. Brostow, R. Chiu, I.M. Kalogeras, A. Vassilikou-Dova, Mater. Lett. **62**, 3152 (2008)
C. Bucci, R. Fieschi, G. Guidgi, Phys. Rev. **148**, 816 (1966)
D.E. Buerger, R.H. Boyd, Macromolecules **22**, 2649 (1989)

D. Cangialosi, G.A. Schwartz, A. Alegria, J. Colmenero, J. Chem. Phys. **123**, 144908 (2005)
D. Cangialosi, A. Alegria, J. Colmenero, Macromolecules **39**, 7149 (2006)
D. Cangialosi, A. Alegria, J. Colmenero, Phys. Rev. E. **76**, 011514 (2007)
P. Cebe, P. Huo, Thermochim. Acta. **238**, 229 (1994)
I. Cendoya, A. Alegria, J.M. Alberti, J. Colmenero, H. Grimm, D. Richter, B. Frick, Macromolecules **32**, 4065 (1999)
F.V. Chávez, K. Saalwächter, Phys. Rev. Lett. **104**, 198305 (2010)
G.-C. Chung, J.A. Kornfield, S.D. Smith, Macromolecules **27**, 5729 (1994a)
G.-C. Chung, J.A. Kornfield, S.D. Smith, Macromolecules **27**, 964 (1994b)
R. Clausius, *Die mechanische Wärmelehre*, vol. II (Vieweg und Sohn, Braunschweig, 1879)
J. Coburn, R.H. Boyd, Macromolecules **19**, 2238 (1986)
K.S. Cole, R.H. Cole, J. Chem. Phys. **9**, 341 (1941)
R.E. Collin, *Foundations for Microwave Engineering*, 2nd edn. (McGraw-Hill, New York, 1966)
J. Colmenero, Macromolecules **46**, 5363 (2013)
J. Colmenero, A. Arbe, Soft Matter **3**, 1474 (2007)
J. Colmenero, A. Arbe, A. Alegria, Phys. A. **201**, 447 (1993)
S. Corezzi, E. Campani, A.P. Rolla, S. Capaccioli, D. Fioretto, J. Chem. **111**, 9343 (1999)
C. Dalle-Ferrier, C. Thibierge, C. Alba-Simionesco, L. Berthier, G. Biroli, J.-P. Bouchaud, F. Ladieu, D. L'Hôte, G. Tarjus, Phys. Rev. E. **76**, 041510 (2007)
D.W. Davidson, R.H. Cole, J. Chem. Phys. **18**, 1417 (1950)
D.W. Davidson, R.H. Cole, J. Chem. Phys. **19**, 1484 (1951)
P.G. de Gennes, *Scaling Concepts in Polymer Physics* (Cornell University Press, Ithaca New York, 1979)
P. Debye, *Polar Molecules, Chemical Catalog*, reprinted by (Dover, New York, 1929)
P. Debye, F. Bueche, J. Chem. Phys. **7**, 589 (1951)
R. Diaz-Calleja, Macromolecules **33**, 8924 (2000)
M.C.S. Dionisio, J.J.M. Ramos, A.C. Fernandes, J. Appl. Polym. Sci. **60**, 903 (1996)
M. Dionissio, A.C. Fernandes, J.F. Mano, N. Correia, R.C. Sousa, Macromolecules **33**, 1002 (2000)
M. Doi, S.F. Edwards, *The Theory of Polymer Dynamics* (Clarendon, Oxford, 1986)
E.J. Donth, J. Non-Cryst. Solids. **53**, 325 (1982)
E.J. Donth, *Relaxation and Thermodynamics in Polymers, Glass Transition* (Akademie Verlag, Berlin, 1992)
E.J. Donth, *The Glass Transition: Relaxation Dynamics in Liquids and Disordered Materials* (Springer, Berlin, 2001)
E.J. Donth, E. Hempel, C. Schick, J. Phys. Cond. Mat. **12**, L281 (2001a)
E.J. Donth, H. Huth, M. Beiner, J. Phys. Cond. Mat. **13**, L451 (2001b)
J.C. Dyre, J. Appl. Phys. **64**, 2456 (1988)
J.C. Dyre, T.B. Schroder, Rev. Mod. Phys. **72**, 873 (2000)
H. Eklind, F.H.J. Maurer, P.A.M. Steeman, Polymer **38**, 1047 (1997)
J.D. Ferry, *Viscoelastic Properties of Polymers*, 3rd edn. (Wiley, New York, 1980)
E.W. Fischer, G.P. Hellmann, H.W. Spiess, F.J. Horth, U. Ecarius, B. Wehrle, Macromol. Chem. Macromol. Chem. Phys. **S12**, 189 (1985)
J.P. Flory, *Statistical Mechanics of Chain Molecules* (Hanser Verlag, München, 1989)
G. Floudas, Effect of pressure on the dielectric spectra of polymeric systems (Chapter 8), in *Broadband Dielectric Spectroscopy*, ed. by F. Kremer, A. Schönhals (Springer, Berlin, 2003)
G. Floudas, M. Paluch, A. Grzybowski, K.L. Ngai, *Pressure Effects on Polymer Blends in Molecular Dynamics of Glass-forming Systems* (Springer, Berlin, 2011)
H. Fröhlich, *Theory of Dielectric* (Oxford University Press, London, 1958)
G.S. Fulcher, J. Am. Ceram. Soc. **8**, 339 (1925)
R.M. Fuoss, J.G. Kirkwood, J. Am. Chem. Soc. **63**, 385 (1941)
G. Schaumburg Dielectric Newsletter of Novocontrol, issue March (1994)
G. Schaumburg Dielectric Newsletter of Novocontrol, issue May (1999)
C. Gainaru, R. Böhmer, Macromolecules **42**, 7616 (2009)

P. Gallo, Phys. Chem. Chem. Phys. **2**, 1607 (2000)
F. Garwe, A. Schönhals, M. Beiner, K. Schröter, E. Donth, Macromolecules **29**, 247 (1996)
J.L. Gomes Ribelles, R.J. Diaz Calleja, J. Polym. Sci. Polym. Polym. Phys. Ed. **23**, 1297 (1985)
W. Götze, *Complex Dynamics of Glass-forming Liquids – A Mode-Coupling Theory* (Oxford University Press, Oxford, 2009)
C. Hall, E. Helfand, J. Chem. Phys. **77**, 3275 (1982)
L. Hardy, I. Stevenson, G. Boiteux, G. Seytre, A. Schönhals, Polymer **42**, 5679 (2001)
S.J. Havriliak, *Dielectric and Mechanical Relaxations in Materials* (Hanser Publishers, Munich, 1997)
S. Havriliak, S. Negami, J. Polym. Sci. Part C **16**, 99 (1966)
S. Havriliak, S. Negami, Polymer **8**, 161 (1967)
T. Hayakawa, K. Adachi, Macromolecules **33**, 6834 (2000a)
T. Hayakawa, K. Adachi, Macromolecules **33**, 6840 (2000b)
D. Hayward, R.A. Pethrick, T. Siriwittayakorn, Macromolecules **25**, 1480 (1992)
Y.Y. He, T.R. Lutz, M.D. Ediger, J. Chem. Phys. **119**, 9956 (2003)
P. Hedvig, *Dielectric Spectroscopy of Polymers* (Adam Hilger, Bristol, 1977)
J. Heijboer, in *Moelecular Basis of Transition and Relaxation*, ed. by D.J. Meier (Gordon and Breach Science Publishers, New York, 1978)
E. Hempel, M. Beiner, T. Renner, E. Donth, Acta. Polym. **47**, 525 (1996)
E. Hempel, G. Hempel, A. Hensel, C. Schick, E.J. Donth, J. Phys. Chem. B **104**, 2460 (2000)
D. Herrera, J.C. Zamora, A. Bello, M. Grimau, E. Laredo, A.J. Müller, T.P. Lodge, Macromolecules **38**, 5109 (2005)
Hewlett Packard Product Note 8510-3 (1985) Measuring the dielectric constant of solids with the HP8510 network analyzer
Y. Hirose, O. Urakawa, K. Adachi, Macromolecules **36**, 3699 (2003)
S. Hoffman, L. Willner, D. Richter, A. Arbe, J. Colmenero, B. Farago, Phys. Rev. Lett. **85**, 772 (2000)
S. Hoffman, D. Richter, A. Arbe, J. Colmenero, B. Farago, Appl. Phys. A. **74**, S442 (2002)
A. Hofmann, F. Kremer, E.W. Fischer, Phys. A. **201**, 106 (1993)
B.S. Hsiao, B.B. Sauer, J. Polym. Sci. Polym. Phys. Ed. **31**, 901 (1993)
S.D. Hudson, D.D. Davis, A.J. Lovinger, Macromolecules **25**, 1759 (1992)
P. Huo, P. Cebe, J. Polym. Sci. Phys. Ed. **30**, 239 (1992a)
P. Huo, P. Cebe, Macromolecules **25**, 902 (1992b)
P. Huo, P. Cebe, Polymer **34**, 696 (1993)
G.Q. Jiang, W.H. Wong, E.Y. Raskovida, W.G. Clark, W.A. Hines, J. Sanny, Rev. Sci. Instrum. **64**, 1614 (1993)
X. Jin, S. Zhang, J. Runt, Macromolecules **37**, 8110 (2004)
G.P. Johari, J. Chem. Phys. **28**, 1766 (1973)
G.P. Johari, M.J. Goldstein, J. Chem. Phys. **53**, 2372 (1970)
S. Kahle, J. Korus, E. Hempel, R. Unger, S. Höring, K. Schröter, E.J. Donth, Macromolecules **30**, 7214 (1997)
D.S. Kalika, R.K. Krishnaswamy, Macromolecules **26**, 4252 (1993)
S. Kamath, R.H. Colby, S.K. Kumar, K. Karatasos, G. Floudas, G. Fytas, J.E.L. Roovers, J. Chem. Phys. **111**, 6121 (1999)
S. Kamath, R.H. Colby, S.K. Kumar, Macromolecules **36**, 8567 (2003a)
S. Kamath, R.H. Colby, S.K. Kumar, Phys. Rev. E. **67**, 010801 (R) (2003b)
R. Kant, S.K. Kumar, R.H. Colby, Macromolecules **36**, 10087 (2003)
F.E. Karasz (ed.), *Dielectric Properties of Polymers* (Plenum, New York, 1972)
K. Karatasos, G. Valaachos, D. Vlassopoulos, G. Fytas, G. Meier, A. Du Chesne, J. Chem. Phys. **108**, 5997 (1998)
G. Katana, A. Zetsche, F. Kremer, E.W. Fischer, ACS Polym. Preprints **33**, 122 (1992)
G. Katana, F. Kremer, E.W. Fischer, R. Plaetscke, Macromolecules **26**, 3075 (1993)
G. Katana, E.W. Fischer, T. Hack, V. Abetz, F. Kremer, Macromolecules **28**, 2714 (1995)

J.G. Kirkwood, J. Chem. Phys. **58**, 911 (1939)
J.G. Kirkwood, Ann. NY Acad. Sci. **40**, 315 (1940)
J.G. Kirkwood, Trans. Faraday Soc. **42A**, 7 (1946)
S. Koizumi, J. Polym. Sci. Polym. Phys. Ed. **42**, 3148 (2004)
F. Kremer, A. Schönhals, *Broadband Dielectric Spectroscopy* (Springer, Berlin, 2003)
F. Kremer, A. Schönhals, Broadband dielectric measurement techniques (Chapter 2), in *Broadband Dielectric Spectroscopy*, ed. by F. Kremer, A. Schönhals (Springer, Berlin, 2003b), pp. 35–58
F. Kremer, A. Hofmann, E.W. Fischer, ACS-Polym. Preprints **33**, 96 (1992)
E. Krygier, G. Lin, J. Mendes, G. Mukandela, D. Azar, A.A. Jones, J.A. Pathak, R.H. Colby, S. Kumar, G. Floudas, R. Krishnamoorti, R. Faust, Macromolecules **38**, 7721 (2005)
U. Kubon, R. Schilling, J.H. Wendorf, Colloid Polym. Sci. **266**, 123 (1988)
A.S. Kulik, H.W. Beckham, K. Schmidt-Rohr, D. Radloff, U. Pawelzik, C. Boeffel, H.W. Spiess, Macromolecules **27**, 4746 (1994)
S.K. Kumar, Macromolecules **33**, 5285 (2000)
S.K. Kumar, R.H. Colby, S.H. Anastasiadis, G. Fytas, J. Chem. Phys. **105**, 3777 (1996)
L.K.H. van Beek Dielectric behavior of heterogeneous systems, in *Progress in Dielectrics*, vol. 7, ed. by J.B. Birks (Heywood, 1967), pp. 69–114
L.D. Landau, E.M. Lifschitz, *Statistical Physics*. Textbook of Theoretical Physics, vol. V (Akademie-Verlag, Berlin, 1979)
C. Larvergne, C. Lacabanne, IEEE Elec. Insul. Mag. **9**, 5 (1993)
E. Leroy, A. Alegria, J. Colmenero, Macromolecules **35**, 5587 (2002)
E. Leroy, A. Alegria, J. Colmenero, Macromolecules **36**, 7280 (2003)
H.S. Li, W. Kim, Polymer **38**, 2657 (1997)
A.E. Likhtman, T.C.B. McLeish, Macromolecules **35**, 6332 (2002)
J.E.M. Lipson, Macrom. Theory Simul. **7**, 263 (1998)
J.E.M. Lipson, M. Tambasco, K.A. Willets, J.S. Higgins, Macromolecules **36**, 2977 (2003)
C.-Y. Liu, R. Keunings, C.D. Bailly, Phys. Rev. Lett. **97**, 246001 (2006)
T.P. Lodge, T.C.B. McLeish, Macromolecules **33**, 5278 (2000)
T.P. Lodge, E.R. Wood, J.C. Haley, J. Polym. Sci. Polym. Phys. Ed. **44**, 756 (2006)
H.A. Lorentz, Ann. Phys. **9**, 641 (1879)
C. Lorthioir, A. Alegria, J. Colmenero, Phys. Rev. E. **86**, 031805 (2003)
X. Lu, R.A. Weiss, Macromolecules **25**, 3242 (1992)
T.R. Lutz, Y.Y. He, M.D. Ediger, Macromolecules **38**, 9826 (2005)
T. Malik, R.E. Prud'homme, Polym. Eng. Sci. **24**, 144 (1984)
J. Maranas, Curr. Opin. Colloid Interface Sci. **12**, 29 (2007)
P.F. Massotti, Bibl. Univ. Modena **6**, 193 (1847)
M. Matsuo, Y. Ishida, K. Yamafuji, M. Takayanagi, F. Irie, Kolloid-Z und Z für Polymere **201**, 7 (1965)
J.C. Maxwell, Phil. Trans. **155**, 459 (1865)
J.C. Maxwell, Phil. Trans. **158**, 643 (1868)
N.G. McCrum, B.E. Read, G. Williams, *Anelastic and Dielectric Effects in Polymeric Solids* (Wiley, New York, 1967) (reprinted by Dover Publications 1991)
D. Migahed, T. Fahmy, Polymer **35**, 1688 (1994)
S.T. Milner, T.C.B. McLeish, Phys. Rev. Lett. **81**, 725 (1998)
N. Miura, W. MacKnight, S. Matsuoka, F.E. Karasz, Polymer **40**, 6129 (2001)
Y. Miwa, K. Usami, M. Yamamoto, T. Sakaguchi, M. Sakai, S. Shimada, Macromolecules **38**, 2355 (2005)
E. Montroll, G.H. Weiss, J. Math. Phys. **6**, 167 (1965)
K. Mpoukouvalas, G. Floudas, Macromolecules **41**, 1552 (2008)
K. Mpoukouvalas, G. Floudas, S. Zhang, J. Runt, Macromolecules **38**, 552 (2005)
T. Nakajima, *Annual Report, Conference on Electrical Insulation and Dielectric Phenomena* (National Academy of Sciences, Washington, DC, 1971)

H. Namikawa, J. Non-Cryst. Solids **18**, 173 (1975)
K.L. Ngai, C.M. Roland, Macromolecules **37**, 2817 (2004)
L. Onsager, J. Am. Chem. Soc. **58**, 1486 (1938)
J.A. Pathak, R.H. Colby, G. Floudas, R. Jerome, Macromolecules **32**, 2353 (1999)
K. Pathmanathan, G.P. Johari, J.P. Faivre, L. Monnerie, J. Polym. Sci. **24**, 1587 (1986)
R. Pelster, IEEE Trans. Microw. Theory Tech. **43**, 1494 (1995)
B.T. Poh, K. Adachi, T. Kotaka, Macromolecules **29**, 6317 (1996)
J. Pugh, T. Ryan, IEE Conf. Dielectric Mater. Meas. Appl. **177**, 404 (1979)
M. Rabeony, D.J. Lohse, R.T. Garnert, S.J. Ham, W.W. Graessley, K.B. Migler, Macromolecules **31**, 6511 (1998)
G.S. Rellick, J. Runt, J. Polym. Sci. Polym. Phys. Ed. **24**, 279 (1986a)
G.S. Rellick, J. Runt, J. Polym. Sci. Polym. Phys. Ed. **24**, 313 (1986b)
G.S. Rellick, J. Runt, J. Polym. Sci. Polym. Phys. Ed. **26**, 1425 (1988)
E. Riande, R. Diaz-Calleja, *Electrical Properties of Polymers* (Marcel Dekker, New York, 2004)
E. Riande, E. Saiz, *Dipole Moments and Birefringence of Polymers* (Prentice Hall, Englewood Cliffs, 1992)
C.M. Roland, K. Ngai, Macromolecules **24**, 2261 (1991)
C.M. Roland, K. Ngai, J. Rheol. Acta. **36**, 1691 (1992a)
C.M. Roland, K. Ngai, Macromolecules **25**, 363 (1992b)
C.M. Roland, S. Hensel-Bielowka, M. Paluch, R. Casalini, Rep. Prog. Phys. **68**, 1405 (2005)
C.M. Roland, K.J. MacGrath, R. Cassalini, Macromolecules **39**, 3581 (2006)
P.E. Rouse, J. Chem. Phys. **21**, 1272 (1953)
W. Ruland, Prog. Colloid Polym. Sci. **57**, 192 (1957)
J.P. Runt, Dielectric studies of polymer blends, in *Dielectric Spectroscopy of Polymeric Materials*, ed. by J.P. Runt, J.J. Fitzgerald (ACS-books, Washington, DC, 1997), pp. 283–302
J.P. Runt, J.J. Fitzgerald (eds.), *Dielectric Spectroscopy of Polymeric Materials* (American Chemical Society, Washington, DC, 1997)
J. Runt, C.A. Barron, Z.-F. Zhang, S.K. Kumar, Macromolecules **24**, 3466 (1991)
T. Sakaguchi, N. Taniguchi, O. Urakawa, K. Adachi, Macromolecules **38**, 422 (2005)
S. Salaniwal, R. Kant, R.H. Colby, S.K. Kumar, Macromolecules **35**, 9211 (2002)
H. Sasabe, S. Saito, J. Polym. Sci. Part A-2 **6**, 1401 (1968)
B.B. Sauer, B.S. Hsiao, J. Polym. Sci. Poly. Phys. Ed. **31**, 917 (1993)
B.B. Sauer, P. Avakian, G.M. Cohen, Polymer **33**, 2666 (1992)
B.B. Sauer, P. Avakian, E.A. Flexman, M. Keating, B.S. Hsiao, R.K. Verma, J. Polym. Sci. Polym. Phys. Ed. **35**, 2121 (1997)
B. Schartel, J.H. Wendorff, Polymer **36**, 899 (1995)
C. Schick, Calorimetry (Chapter 2.31), in *Polymer Science: A Comprehensive Reference*, vol. 2, ed. by K. Matyjaszewski, M. Möller (Elsevier, Amsterdam, 2012), pp. 793–823
E. Schlosser, A. Schönhals, Colloid Polym. Sci. **267**, 963 (1989)
K. Schneider, A. Schönhals, E.J. Donth, Acta Polym. **32**, 471 (1981)
A. Schönhals, Macromolecules **26**, 1309 (1993)
A. Schönhals, Europhys. Lett. **56**, 815 (2001)
A. Schönhals, Molecular dynamics in Polymeric model systems (Chapter 7), in *Broadband Dielectric Spectroscopy*, ed. by F. Kremer, A. Schönhals (Springer, Berlin, 2003)
A. Schönhals, F. Kremer, J. Non-cryst. Solids **172–174**, 336 (1994)
A. Schönhals, F. Kremer, Analysis of dielectric spectra (Chapter 3), in *Broadband Dielectric Spectroscopy*, ed. by F. Kremer, A. Schönhals (Springer, Berlin, 2003a), pp. 59–98
A. Schönhals, F. Kremer, Theory of dielectric relaxation (Chapter 1), in *Broadband Dielectric Spectroscopy*, ed. by F. Kremer, A. Schönhals (Springer, Berlin, 2003c)
A. Schönhals, E. Schlosser, Colloid Polym. Sci. **267**, 125 (1989)
A. Schönhals, H. Goering, C. Schick, B. Frick, R. Zorn, J. Non-cryst. Solids **351**, 2668 (2005)

A. Schönhals, F. Kremer, Amorphous polymers (Chapter 1.08), in *Polymer Science: A Comprehensive Reference*, vol. 1, ed. by K. Matyjaszewski, M. Möller (Elsevier, Amsterdam, 2012), pp. 201–226
S. Schrader, A. Schönhals, Prog. Colloid Polym. Sci. **80**, 93 (1989)
K. Schröter, R. Unger, S. Reissig, F. Garwe, S. Kahle, M. Beiner, E. Donth, Macromolecules **31**, 8966 (1998)
G.A. Schwartz, A. Alegria, J. Colmenero, J. Chem. Phys. **127**, 154907 (2007a)
G.A. Schwartz, J. Colmenero, A. Alegria, Macromolecules **40**, 3246 (2007b)
K. Se, O. Takayanagi, K. Adachi, Macromolecules **30**, 4877 (1997)
A. Serghei, M. Tress, J.R. Sangoro, F. Kremer, Phys. Rev. B **80**, 184301 (2009)
T.F. Shatzki, J. Polym. Sci. **57**, 496 (1962)
S. Shenogin, R. Kant, R.H. Colby, S.K. Kumar, Macromolecules **40**, 5767 (2007)
R.W. Sillars, J. Inst. Elect. Eng. **80**, 378 (1937)
G.P. Simon, A. Schönhals, Dielectric relaxation and thermal stimulated currents, in *Polymer Characterization Techniques and Their Application to Blends*, ed. by G.P. Simon (Oxford University Press, Oxford/New York, 2003), pp. 96–131
J. Skolnik, R. Yaris, Macromolecules **15**, 1041 (1982)
L.H. Sperling, *Introduction to Physical Polymer Science* (Wiley, New York, 1986)
P.A.M. Steeman, F.H.J. Maurer, Colloid Polym. Sci. **268**, 315 (1990)
P.A.M. Steeman, F.H.J. Maurer, Colloid Polym. Sci. **270**, 1069 (1992)
P.A.M. Steeman, J. van Turnhout, Dielectric properties of inhomogeneous media (Chapter 13), in *Broadband Dielectric Spectroscopy*, ed. by F. Kremer, A. Schönhals (Springer, Berlin, 2003), pp. 495–522
P.A.M. Steeman, F.H.J. Maurer, J. van Turnhout, Polym. Eng. Sci. **34**, 697 (1994)
W.H. Stockmayer, Pure Appl. Chem. **15**, 539 (1967)
W.H. Stockmayer, J.J. Burke, Macromolecules **2**, 647 (1969)
G.R. Strobl, *The Physics of Polymers* (Springer, Heidelberg, 1996)
J. Swenson, R. Bergman, S. Longeville, J. Chem. Phys. **115**, 1299 (2001)
J.W. Sy, J. Mijovic, Macromolecules **33**, 933 (2000)
M. Tambasco, J.E.M. Lipson, J.S. Higgins, Macromolecules **39**, 4860 (2006)
G. Tammann, W. Hesse, Z. Anorg. Allg. Chem. **156**, 245 (1926)
T. Tetsutani, M. Kakizaki, T. Hideshima, Polym. J. **14**, 305 (1982a)
T. Tetsutani, M. Kakizaki, T. Hideshima, Polym. J. **14**, 471 (1982b)
G. Teyssedre, S. Mezghani, A. Bernes, C. Lacabanne, in *Thermally Stimulated Currents of Polymers in Dielectric Spectroscopy of Polymeric Materials*, ed. by J. Runt, J.J. Fitzgerald (ACS, Washington, DC, 1997), pp. 227–258
M. Topic, Z. Veksli, Polymer **34**, 2118 (1993)
M. Topic, A. Mogus-Milankovic, Z. Katovic, Polymer **28**, 33 (1987)
G. Turky, D. Wolff, A. Schönhals, Macromol. Chem. Phys. **22**, 2420 (2012)
M. Tyagi, A. Arbe, J. Colmenero, B. Frick, J.R. Stewart, Macromolecules **39**, 3007 (2006)
M. Tyagi, A. Arbe, A. Alegria, J. Colmenero, B. Frick, Macromolecules **40**, 4568 (2007)
O. Urakawa, K. Adachi, T. Kotaka, Macromolecules **26**, 2036 (1993a)
O. Urakawa, K. Adachi, T. Kotaka, Macromolecules **26**, 2042 (1993b)
O. Urakawa, Y. Fuse, H. Hori, Q. Tran-Cong, O. Yano, Polymer **42**, 765 (2001)
O. Urakawa, T. Sugihara, K. Adachi, Polym. Appl. (Japan) **51**, 10 (2002)
O. Urakawa, T. Ujii, K. Adachi, J. Non-cryst. Solids **352**, 5042 (2006)
B. Valeur, J.P. Jarry, F. Geny, J. Monnerie, J. Polym. Sci. Polym, Polym. Phys. Ed. **13**, 667 (1975a)
B. Valeur, J. Monnerie, J.P. Jarry, J. Polym. Sci. Polym. Phys. Ed. **13**, 675 (1975b)
J. van Turnhout, *Thermally Stimulated Discharge of Polymer Electrets* (Elevier, Amsterdam, 1975)
J. Vanderschueren, M. Landang, J.M. Heuschen, Macromolecules **13**, 973 (1980)
H. Vogel, Phys. Z. **22**, 645 (1921)

M.V. Volkenstein, *Configurational Statistics of Polymeric Chains* (Wiley Interscience, New York, 1963)
R.W. Wagner, Arch. Elektrotech. **2**, 371 (1914)
H. Watanabe, M. Yamazaki, H. Yoshida, K. Adachi, T. Kotaka, Macromolecules **24**, 5365 (1991)
H. Watanabe, O. Urakawa, H. Yamada, M.-L. Yao, Macromolecules **29**, 755 (1996)
R.E. Wetton, W.J. MacKnight, J.R. Fried, F.E. Karasz, Macromolecules **11**, 158 (1978)
G. Williams, Adv. Polym. Sci. **33**, 60 (1979)
G. Williams, D.A. Edwards, Trans. Faraday Soc. **62**, 1329 (1966)
G. Williams, D.C. Watts, Trans. Faraday Soc. **67**, 2793 (1971)
G. Williams, in *Comprehensive Polymer Science*, vol. II, ed. by G. Allen, J.C. Bevington (Pergamon Press, Oxford, 1989)
G. Williams, in *Structure and Properties of Polymers*, ed. by E.L. Thomas. Materials Science & Technology Series, vol. 12 (Wiley and Sons, Hoboken, New Jersey, 1993), p. 471
B. Wunderlich, Prog. Polym. Sci. **28**, 383 (2003)
H. Yin, S. Napolitano, A. Schönhals, Macromolecules **45**, 1652 (2012)
M. Zamponi, A. Wischnewski, M. Monkenbusch, L. Willner, D. Richter, A.E. Likhtman, G. Kali, B. Farago, Phys. Rev. Lett. **96**, 238302 (2006)
S. Zeeb, S. Höring, F. Garwe, M. Beiner, A. Schönhals, K. Schröter, E. Donth, Polymer **38**, 4011 (1997)
A. Zetsche, E.W. Fischer, Acta Polym. **45**, 168 (1994)
A. Zetsche, F. Kremer, H. Jung, Polymer **31**, 1883 (1990)
S. Zhang, X. Jin, P.C. Painter, J. Runt, Macromolecules **38**, 6216 (2005)
R. Zorn, L. Hartmann, B. Frick, D. Richter, Kremer F **307**, 547 (2002)